LBL-7723

THE NUCLEAR AND ATOMIC PHYSICS GOVERNING CHANGES IN THE COMPOSITION OF RELATIVISTIC COSMIC RAYS

Lance W. Wilson
(Ph. D. thesis)

May 1978

Prepared for the U. S. Department of Energy
under Contract W-7405-ENG-48

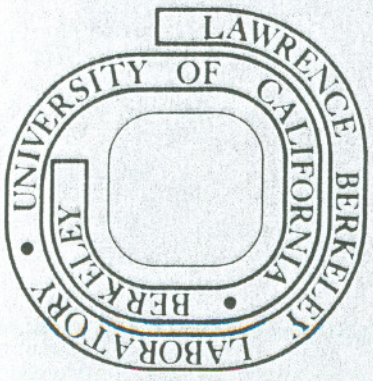

THE NUCLEAR AND ATOMIC PHYSICS GOVERNING CHANGES IN THE COMPOSITION OF RELATIVISTIC COSMIC RAYS

Lance W. Wilson
Lawerence Berkeley Laboratory

This work was supported by the U. S. Department of Energy.

DEDICATION

To all who wondered about not only when but if, especially Eileen, Brett, and Sage.

ABSTRACT

Many quantitative studies of relativistic cosmic ray propagation exist in which "standard" values for the input quantities are adopted in an uncritical manner. In contrast, the major emphasis of this study is on developing the proper set of formulae and error estimates for each of the atomic and nuclear processes that govern the composition of the cosmic rays between lithium and nickel. In particular, it is shown that errors of approximately a factor of two exist in the standard (Bohr) cross sections for stripping, that the correction function from high energy photoionization needs to be introduced into the standard cross section for radiative attachment, and that because the half-life of a fast nucleus with at most one K-shell electron can differ from the half-life of a neutral atom, several laboratory-based values need correction. The framework used to assemble and correct these quantities is a matrix formalism for the leaky box model similar to that used by Cowsik and Wilson in their "nested leaky box" model. It is shown that once the assumption of species-independent leakage is introduced, the matrix formalism becomes virtually identical with the standard exponential path length formalism.

INTRODUCTION

The measurement of the charge composition and energy spectra of relativistic cosmic rays permits a quantitative study of their origin and propagation. Once the effects of interactions with the interstellar medium are removed, the composition at the source can be compared to the predictions of models. Thus, it is important to include those processes that can change the composition from its source value. For some elements, the difference between the charge composition at the source and at the top of the atmosphere can be quite dramatic. The elements Li, Be, and B provide a classic example of this difference. At the top of the atmosphere the ratio (Li + Be + B)/(C + O) is quite large (≈ 0.25) and yet spectroscopic observations (cf. Cameron 1973 and Meyer and Reeves 1977) and the fact that all three elements are destroyed in stellar interiors with $T \geq 10^6$K indicate that the same ratio should be ≈ 0 at the source.

The assumption that the abundances of Li, Be, and B at the top of the atmosphere reflect the effects of the intervening medium has been used in all models for cosmic ray propagation. The original equilibrium model of Bradt and Peters (1950) sought to explain their abundances in terms of the cross sections for production from the fragmentations of such heavier parent nuclei as C and O. When that model predicted too much Li, Be, and B (relative to C and O), their abundances were used to determine the mean amount of intervening matter. The concept of using one thickness for the slab of intervening

matter was most fully developed by Fichtel and Reames (1966) and came to be called the slab model. When a single thickness failed to explain both the abundances of Li, Be, and B and the abundances of the elements in the range $19 \leq Z \leq 25$, the slab model was extended to the exponential path-length model by Cowsik et al. (1967). In this model the abundances of Li, Be, and B were used to determine the mean matter thickness. This model was given a better theoretical justification and the new name of the "leaky box" model by Gloeckler and Jokipii (1969). Once again, the abundances of Li, Be, and B were used to determine the mean amount of matter traversed by primaries before "leaking out of the Galaxy."

For the elements between lithium and nickel many quantitative studies of cosmic ray propagation exist (Shapiro et al. 1975, Garcia-Munoz et al. 1977, Raisbeck and Yiou 1977, Hagen et al. 1977, Webber et al. 1977) in which "standard" values for the input quantities are adopted in an uncritical manner. In contrast, in this study the major emphasis is on developing the proper set of formulae for the atomic and nuclear processes that govern the composition. In particular, errors in the standard rates of decay of unstable nuclei and in the cross sections for the attachment and stripping of atomic electrons are pointed out and corrected.

The framework used to assemble and correct the input quantities is a matrix formalism for the standard leaky box model that is similar to that used by Cowsik and Wilson (1973, 1975) in their "nested leaky box" model. The major difference is that the "nested leaky box" model requires a product of two modification matrices (one for each

confinement region), while in this work only a single modification matrix is required. In addition, this work provides a much more detailed discussion of how the matrix formalism connects with other methods and shows how to obtain the minimal set of isotopes that requires explicit treatment.

I. Matrix Formulation

(a) General considerations

The basic transport equation for cosmic ray nuclei is a second order partial differential equation (cf. Ginzburg and Syrovatskii 1964). However, if one imagines that the nuclei are confined in some region within which they are uniformly distributed and such that their frequent encounters with the boundary have a low probability for escape, their transport equation becomes somewhat simplified. Further simplification is possible at energies above 1 GeV/nucleon because the processes of energy loss and solar modulation have a negligible effect. In particular, the equation for cosmic ray nuclei that incorporates the change with time of the differential number density $N_{(Z,A,z)}(T)$ of particles having kinetic energies per nucleon between T and T + dT that also have atomic number Z, mass number A, and net charge z is given by (cf. Gloeckler and Jokipii 1969; Cowsik and Wilson 1973, Eq. [2.1]) the expression

$$\frac{dN_{(Z,A,z)}(T)}{dt} = \frac{1}{\tau_{(Z,A,z)}} N_{(Z,A,z)} - n_H \sigma_{(Z,A)} v N_{(Z,A,z)}$$

$$+ \sum_{(Z',A')} n_H \int \sigma_{(Z,A),(Z',A')}(T,T') v' N_{(Z',A',z')}(T') dT'$$

$$+ S_{(Z,A,z)} - \frac{1}{\gamma\tau^*_{(Z,A,z)}} N_{(Z,A,z)} + \sum_{(Z'',A'')} \frac{1}{\gamma\tau^*_{(Z'',A'',z'')}} N_{(Z'',A'',z'')} \qquad (1)$$

$$- n_H \sigma^{att}_{(Z,A,z)} v N_{(Z,A,z)} - n_H \sigma^{strip}_{(Z,A,z)} v N_{(Z,A,z)}$$

$$+ n_H \sigma^{att}_{(Z,A,z+1)} v N_{(Z,A,z+1)} + n_H \sigma^{strip}_{(Z,A,z-1)} v N_{(Z,A,z-1)} \quad (1)$$

where

T is the kinetic energy per nucleon;

$1/\tau_{(Z,A,z)}$ is the leakage probability per unit time for (Z,A,z);

n_H is the number density of hydrogen in the containment volume;

$\sigma_{(Z,A)}$ is the reaction (or inelastic) cross section per hydrogen atom at energy T;

$\sigma_{(Z,A),\,(Z',A')}(T,T')$ is the partial cross section per hydrogen atom per unit energy interval for the formation of a nucleus (Z,A) at energy T from the interaction of a projectile nucleus of (Z',A') and energy T';

$S_{(Z,A,z)}$ is the differential source injection rate per unit volume at the energy T;

v is the velocity;

γ is the Lorentz factor $(1 - v^2/c^2)^{-\frac{1}{2}}$;

c is the velocity of light;

$\tau_{*(Z,A,z)}$ is the mean-life (not half-life) for radioactive decay in the rest frame of a nucleus (Z,A) that has Z-z electrons attached;

$\sigma^{att}_{(Z,A,z)}$ is the cross section per hydrogen atom at the energy T for an electron attachment by a nucleus (Z,A) that reduces its net charge from z to z-1 (0 if z = 0);

$\sigma^{strip}_{(Z,A,z)}$ is the cross section per hydrogen atom at the energy T for stripping an electron off a nucleus (Z,A) and increasing its net charge from z to z+1 (0 if z = Z).

Note that the first three terms of Eq. (1) represent leakage losses, interaction losses, and interaction gains, respectively. If (Z,A) is an unstable parent nucleus, the fifth term represents losses due to radioactive decays. If (Z,A) is a daughter nucleus, the sixth term represents its gains through radioactive decays. Although not normally included, the last four terms incorporate the atomic processes that govern the net charge. That is, the seventh (eighth) terms represent the losses due to an increase (decrease) in the number of electrons attached. Similarly, the last two terms represent gains because of an increase or decrease in the number of electrons attached. These last four terms become important for nuclei that can decay via electron capture.[1] Lastly, note that it is common to introduce the definitions

$$x = m_H n_H vt,$$

$$x_0 = m_H n_H v\tau \qquad (2)$$

[1]Throughout this work, the term electron capture will be used to mean the nuclear decay process. The term electron attachment will be used to mean the atomic process by which an electron becomes bound to a nucleus.

into Eq. (1), where m_H is the mass of a hydrogen atom. However, this substitution is not useful whenever, as in this work, long-lived decays are to be explicitly included in the formalism.

It is common to make two further approximations before using Eq. (1). The first is to assume that those events in which the cosmic ray suffers an inelastic collision, but remains intact, constitute a negligible fraction of the total reaction cross section, or equivalently, that the fragmentation cross section is approximately equal to the reaction cross section. More explicitly, in this work it will be assumed that

$$\left(\int \sigma_{(Z,A),(Z,A)}(T,T')\, dT' \right) / \sigma_{(Z,A)}(T) \ll 1 \quad , \tag{3}$$

where the numerator is just the cross section for inelastic-yet-intact events. The second approximation stems from the fact that for projectiles and fragments with $A \geq 5$, the fragments have very nearly the same velocity as the projectile (cf. Heckman et al. 1972 and Greiner et al. 1975). This means that the differential cross section, $\sigma_{(Z,A),(Z',A')}(T,T')$, is concentrated at a kinetic energy per nucleon, T, close to that of the projectile. Thus, since this work deals with the elements between Li and Ni, the delta function approximation (Ginzburg and Syrovatskii 1964) which assumes

$$\sigma_{(Z,A),(Z',A')}(T,T') \simeq \sigma_{(Z,A),(Z',A')}\delta(T-T')$$

can be used where $\sigma_{(Z,A),(Z',A')}$ is now the integrated cross section for producing (Z,A). With these approximations, Eq. (1) becomes a simple algebraic relationship describing the transmutations cosmic rays undergo while propagating from the sources. That is, considering the various $N_{(Z,A,z)}$'s and $S_{(Z,A,z)}$'s as components of column vectors, the equation has a matrix form.

Before making an explicit definition of the matrices, it is convenient to introduce some further notation. Let n_{iso} be the total number of species in the propagation analysis. Next, let $\underset{\sim}{N}$ and $\underset{\sim}{S}$ be column vectors of length n_{elem} whose components provide the elemental density and injection rate per unit volume, respectively. That is, $\underset{\sim}{N}$ and $\underset{\sim}{S}$ represent the results of keeping Z fixed and summing over A and z. Also, let ε be the rectangular matrix of dimension n_{iso} by n_{elem} whose (i,j)-th entry contains the fraction of the j-th component of N that belongs to the i-th component of $N_{(Z,A,z)}$. Similarly, let ν be the rectangular matrix of n_{iso} by n_{elem} which expands $\underset{\sim}{S}$ to $S_{(Z,A,z)}$. Thus with these definitions the quantities $N_{(Z,A,z)}$ correspond to the column vectors $\varepsilon\underset{\sim}{N}$ and $\nu\underset{\sim}{S}$, respectively. Strictly speaking, ε and ν are two-dimensional matrices; however, they are also similar to column vectors in that each has a maximum of one non-zero entry per row and the form sketched below:

With the above definitions Eq. (1) can then be written in the more compact form

$$\frac{d}{dt}(\varepsilon \underset{\sim}{N}) = Mv(\varepsilon \underset{\sim}{N}) + \nu \underset{\sim}{S} \tag{5}$$

where in order to permit a rapid conversion from density to flux one power of v has been "removed" from the modification matrix M and where M is the sum of the fragmentation and leakage matrix, F; of the decay matrix, D; and the electron attachment and stripping matrix, E. That is, if $(\varepsilon \underset{\sim}{N})_i$ corresponds to $N_{(Z,A,z)}$ then

$$M_{ij} = F_{ij} + D_{ij} + E_{ij} \tag{6}$$

where

$$F_{ij} = \begin{cases} -\left(\frac{1}{\tau v} + n_H \sigma_{(Z,A)}\right) & \text{, if } i = j \\ n_H \sigma_{(Z,A),(Z',A')} & \text{, if } i \neq j \text{ and } j \text{ corresponds to } (Z',A') \\ 0 & \text{, otherwise} \end{cases} \tag{7}$$

$$D_{ij} = \begin{cases} -\dfrac{1}{\gamma\tau_{*(Z,A,z)}\, v} & \text{, if } i = j,\ (Z,A,z) \text{ unstable} \\ +\dfrac{1}{\gamma\tau_{*(Z'',A'',z'')}\, v} & \text{, if } i \neq j,\ (Z'',A'',z'') \text{ decays to } (Z,A,z) \\ & \quad \text{and } j \text{ corresponds to } (Z'',A'',z'') \\ 0 & \text{, otherwise} \end{cases} \tag{8}$$

$$
\begin{array}{c}
\overbrace{\qquad\qquad\qquad}^{n_{elem}} \\
\left.\begin{array}{c} \\ \\ \\ \\ \\ \\ \\ \\ \end{array}\right\}^{n_{iso}}
\left(\begin{array}{ccccc}
* & 0 & . & . & . \\
* & 0 & . & . & . \\
0 & * & & & \\
0 & * & & & \\
0 & * & & & \\
. & & . & & \\
. & & & . & \\
. & & & & .
\end{array}\right)
\end{array}
$$

where * denotes a non-zero entry.

As will be seen in § I(b) and III, the introduction of the ε and ν arrays permits a clearer distinction between those aspects of a propagation analysis that take place at the species level and those that occur at the element level. Finally, note that because at a given energy/nucleon the sum of all of the fractions must yield unity, ε and ν satisfy the normalization equations

$$\sum_{i=1}^{n_{iso}} \varepsilon_{iK} = 1 \tag{4a}$$

and

$$\sum_{i=1}^{n_{iso}} \nu_{iK} = 1 \tag{4b}$$

for each $K=1,\ldots,n_{elem}$.

$$E_{ij} = \begin{cases} -[n_H \sigma^{att}_{(Z,A,z)} + n_H \sigma^{strip}_{(Z,A,z)}] & , \text{ if } i = j \\ + n_H \sigma^{strip}_{(Z,A,z-1)} & , \text{ if } i \neq j, \text{ j corresponds to } (Z,A,z-1) \\ + n_H \sigma^{att}_{(Z,A,z+1)} & , \text{ if } i \neq j, \text{ j corresponds to } (Z,A,z+1) \\ 0 & , \text{otherwise.} \end{cases} \quad (9)$$

Finally, note that if a steady state has been reached within the confinement region, i.e., if the gains and losses are balanced for each species, then Eq. (5) says

$$Mv \, \varepsilon \, \underset{\sim}{N} + v \underset{\sim}{S} = 0 \quad . \quad (10)$$

(b) Leaky box model

The leaky box model assumes that the entire Galaxy acts as the confinement region and that a steady state has been reached. Once its parameters n_H and $\tau_{(Z,A,z)}$ are specified (or determined), Eq. (10) tells how to derive the isotopic source abundances from the isotopic abundances at the top of the atmosphere.

Of course, most of the present cosmic ray observations above 1 GeV/nucleon provide fluxes at the elemental, not isotopic, level. That is, in the notation of Eq. (10), observations provide a $v\underset{\sim}{N}$, not both ε and $v\underset{\sim}{N}$. Thus, some assumption must be made about the isotope fractions at either the sources or the top of the atmosphere. The typical assumption (Tsao et al. 1973) is that the sources inject fully stripped isotopes and that the isotope fractions at the source (the

non-zero components of the matrix ν) are given by the Cameron (1973) compilation. For example, this assumption would fix the $^{12}C/^{13}C$ and $^{16}O/^{17}O$ ratios at the source at their "universal" values but would not make any assumption about the C/O ratio at the source. Once an assumption for ν has been made, the measurements of $\nu\underset{\sim}{N}$ and the measurements and estimates for the components of M can be used in Eqs. (4) and (10) to solve for ε and $\underset{\sim}{S}$ as a function of the parameters n_H and $\tau_{(Z,A,z)}$.

(c) Connection between matrix and path-length formulations

Since cosmic ray propagation calculations are often discussed in terms of particular path-length distributions, this section will make the connection between the matrix and path-length formulations. First, however, note that as shown below the path-length formulation can treat only those cases in which, at the same kinetic energy per nucleon, the leakage is independent of species. No such restriction occurs in the matrix formulation.

(i) Slab Model

As noted above, the slab model was an early attempt to incorporate the effects of nuclear interactions with the interstellar medium. In this model these effects are obtained via the approximation that all cosmic rays must pass through a single uniform slab of material that neither creates nor "leaks" particles. In this way, Eq. (5) can be treated as an initial value problem for the column vector $\underset{\sim}{\eta} = \varepsilon\underset{\sim}{N}$. That is, $\underset{\sim}{\eta}$ is the unique solution to the problem

$$\begin{cases} \dfrac{d\underset{\sim}{\eta}}{dt} = M'v\,\underset{\sim}{\eta} \quad , \quad \forall\, t>0 \quad , \\ \underset{\sim}{\eta}\,(t=o) = \underset{\sim}{\eta}_o \quad , \end{cases} \tag{11}$$

where M' $(\equiv (M + \frac{1}{\tau v}))$ is the modification matrix without leakage and $\underset{\sim}{\eta}_o$ is the column vector that contains the injection density for each species. At high energies M' is independent of t so that the matrix solution of Eq. (11) is just

$$\underset{\sim}{\eta} = \exp\,(M'vt)\,\underset{\sim}{\eta}_o \quad , \forall\, t \geq 0 \tag{12}$$

where the matrix $\exp\,(M'vt) = \sum_{n=0}^{\infty} (M'vt)^n/n!$.

Equation (12) and measurements of the abundances at the top of the atmosphere can then be used to determine the (constant) time interval, t_s, between the injection and the detection of a cosmic ray. This calculation is done by finding a value t_s such that $[\exp\,(-M'vt_s)\,\underset{\sim}{\eta}\,]_i \approx 0$, if i is any of the isotopes of Li, Be, and B.

As shown by Ginzburg and Syrovatskii (1964), there is an equivalent way of writing Eq. (12) that emphasizes the diagonal terms and the time dependence. This alternate form will be useful for some formal manipulations and is given by the equation

$$\eta_i = A_{ij}\, e^{-d_j t} \quad , \tag{13}$$

where d_j is the diagonal term of M'v and the A_{ij} are recursively defined in terms of the off-diagonal, diagonal, and initial values of the isotopes heavier than the i-th isotope. Explicit values for the A_{ij} are not needed for this work; they are given in Ginzburg and Syrovatskii (1964).

(ii) General Path-Length Formulation

Even if the distribution of times, P(t), between the injection and the detection of cosmic rays is not narrow enough to be approximated by a single value, the observed density can often be written as superposition of solutions to different slab models. That is, if P(t) is species-independent and is normalized such that $\int_0^\infty P(t)dt = 1$, then $\underset{\sim}{\eta}$ is given by (cf. Meneguzzi et al. 1975) the equation

$$\underset{\sim}{\eta} = \int_0^\infty \underset{\sim}{\eta}_S(t)P(t)dt \qquad (14)$$

where $\underset{\sim}{\eta}_S$ is a solution to the slab model equation (11)). Assuming that the sources constantly inject the same initial composition, Eq. (12) can be used so that Eq. (14) becomes

$$\underset{\sim}{\eta} = \left[\int_0^\infty \exp\ (M'vt)P(t)dt\right] \underset{\sim}{\eta}_0 \quad . \qquad (15)$$

Equation (15) gives the most general form for the asymptotic (steady state) cosmic ray density in terms of the distribution P, the elements of M', and the injection composition, $\underset{\sim}{\eta}_0$. Note that it is the requirement that P be a scalar function or, equivalently, the fact that M' is not diagonal that does not permit the path-length to be species-dependent.

(iii) Leaky Box Model

As the name implies, in the leaky box model it is assumed that the distribution of times between injection and detection stems from the confinement region's leakage losses. More specifically, if the leakage rate is a constant, τ, and independent of the previous history of the particle, then the equation

$$P(t) = \tau^{-1} \exp(-t/\tau) \tag{16}$$

gives the properly normalized distribution. This form for P(t) demonstrates why another name for this model is the exponential path-length model.

With this definition of P, Eq. (15) becomes

$$\underset{\sim}{\eta} = \left\{ \int_0^\infty \exp \left[(M' - \frac{1}{\tau} I) vt \right] \quad dt \right\} \underset{\sim}{\eta}_o/\tau \tag{17}$$

where I is the identity matrix. Using the power series definition for the exponential operator, and Eq. (13) for the evaluation at the upper limit, Eq. (17) becomes

$$\underset{\sim}{\eta} = -(M' - \frac{1}{\tau} I)^{-1} \underset{\sim}{\eta}_o/\tau \tag{18}$$

After reintroducing the definitions of ε, $\underset{\sim}{N}$, and M, Eq. (18) becomes

$$M v \varepsilon \underset{\sim}{N} + \underset{\sim}{\eta}_o/\tau = 0 \tag{19}$$

Equation (19) differs from Eq. (10) only in the way the steady state source term is represented. In the matrix formulation (Eq. (10)) it is convenient to think in terms of a source injection rate per unit volume so that the second term is written $\nu \underset{\sim}{S}$; while in the path-length formulation (Eq. (19)) the steady state injection is determined by the equivalent loss rate from the material, i.e., the density at injection of each species divided by the mean time spent in the material. Thus, if the τ of Eq. (10) is independent of species, the matrix formulation becomes equivalent to the exponential path-length formulation.

(iv) Path-Length Distributions in gm/cm^2

Radioactive decays are often treated in the limiting cases of complete survival or instantaneous decay. In these cases, the D matrix (Eq. (8)) does not appear and it becomes convenient to introduce the variables x and x_o (see Eq. (2)) having the units of gm/cm^2. For the leaky box model, these substitutions result in the path-length distribution

$$P(x) = x_o^{-1} \quad \exp(-x/x_o) \quad . \tag{20}$$

II. A Critical Review of Input Quantities

(a) Reducing the Number of Coupled Propagation Equations

In the quite general discussions of § I it was never necessary to specify the actual number of isotopes and charge states that were being explicitly treated by the formalism. The minimum size of the column vectors and matrices can be determined by the requirement that an isotope or charge state be truly "coupled". That is, those isotopes or charge states whose N's (densities) are completely specified by another N do not need to be included in the minimal set of coupled equations.

(i) Can $N_{(Z,A,Z-1)}$ be eliminated?

The first reduction via the above requirement comes from the fact that even though nuclei that are not fully stripped have been included in the propagation equation, the inclusion can affect more than one other N only when the nuclei decay via electron capture. This claim is demonstrated most clearly by writing the steady state equation for a nucleus (Z,A) having one electron attached. Then

$$\frac{dN}{dt}(Z,A,Z-1) = 0 \approx -\frac{N_{(Z,A,Z-1)}}{\gamma\tau_{EC}} - n_H \sigma^{strip}_{(Z,A,Z-1)} \, vN_{(Z,A,Z-1)}$$

$$+n_H \sigma^{att}_{(Z,A,Z)} \, vN_{(Z,A,Z)} \quad , \tag{21}$$

where leakage, spallation, and attachment losses have been neglected relative to the stripping loss, and it is implicitly assumed that the source of cosmic rays injects fully stripped nuclei, that spallation products are fully stripped, that β-decay products are fully stripped, and that the concentration of nuclei with 2 electrons is negligible. Next note that, with the above assumptions, $N_{(Z,A,Z-1)}$ will occur in a maximum of 2 equations other than Eq. (21) - namely the equation for the fully stripped nucleus and, if electron capture is possible, in the equation for the fully stripped end product (Z-1,A). In fact, $N_{(Z,A,Z-1)}$ actually enters into the equation for the fully stripped nucleus in the same combination as the last two terms of Eq. (21) (although with opposite signs). Moreover, Eq. (21) shows that if the nucleus does not decay by electron capture then these two terms would sum to zero. In so doing, however, not only is the occurrence of $N_{(Z,A,Z-1)}$ completely eliminated in the equation for the fully stripped nucleus, but also eliminated is the need to include the charge state in the minimal set of coupled equations.

As discussed by Yiou and Raisbeck (1970), a nucleus that decays by electron capture falls into one of two classes - "spallation" isotopes (if $\gamma\tau_{EC} << \tau_{strip}$) and "clock" isotopes (if $\gamma\tau_{EC} </< \tau_{strip}$) where τ_{strip} is the mean time between electron stripping collisions. For a "spallation" isotope, stripping cannot compete with decay so that an attachment is always followed by that decay. This sequence has two consequences - first, the term in the steady state equation for $N_{(Z,A,Z)}$ which is proportional to $\sigma^{strip}_{(Z,A,Z-1)}$ can be neglected and second, Eq. (21) becomes

$$\frac{N_{(Z,A,Z-1)}}{\gamma\tau_{EC}} = n_H \sigma^{att}_{(Z,A,Z)} vN_{(Z,A,Z)} \quad . \tag{22}$$

Since the left hand side of Eq. (22) also occurs in the steady state equation for (Z-1,A,Z-1), and since the right hand side also occurs in the equation for (Z,A,Z), Eq. (22) can be used to bypass (and thereby eliminate) $N_{(Z,A,Z-1)}$. Note that these substitutions then provide a direct spallation-like coupling of the fully stripped parent nucleus to the fully stripped daughter nucleus that is independent of the mean life for the decay. This somewhat paradoxical result can be understood by nothing that for such an isotope, the rate limiting step for the process is the target density-dependent attachment and not the decay rate of the partially stripped nucleus.

For "clock" isotopes, the decay rate of the partially stripped species does enter into the process and no such simplification is possible. For these isotopes, both the one-electron case and the fully stripped case are truly coupled and must be propagated.

In summary, the standard practice of including only fully stripped nuclei in the minimum set of species is correct for all cases other than "clock" isotopes.

(ii) Eliminating short-lived beta decays

The simplified propagation equation for nuclei with short-lived β^- or β^+ decays also leads to a reduction. If its mean life is sufficiently short, then a particle will decay to a stable (or at least

a long-lived) end product before fragmentation or leakage can take place. For definiteness, assume (Z'',A'') decays to (Z,A) and that its mean life is so short that

$$\frac{1}{\gamma\tau^*_{(Z'',A'')}} >> \frac{1}{\tau_{(Z'',A'',Z'')}} + n_H \sigma_{(Z'',A'')} v \quad . \tag{23}$$

Then the steady state equation for (Z'',A'') becomes

$$0 = \sum_{(Z',A') > (Z'',A'')} n_H \sigma_{(Z'',A''),(Z',A')} vN_{(Z',A',z')} + S_{(Z'',A'',z'')} - \frac{1}{\gamma\tau^*_{(Z'',A'')}} N_{(Z'',A'',z'')} + \sum_{(Z''',A''')} \frac{1}{\gamma\tau^*_{(Z''',A''')}} N_{(Z''',A''',z''')} \tag{24}$$

Incorporating Eq. (24) into the steady state equation for the daughter (Z,A) gives

$$0 = -\frac{1}{\tau_{(Z,A,Z,)}} N_{(Z,A,z)} - n_H \sigma_{(Z,A)} vN_{(Z,A,z)} + \sum_{(Z',A') > (Z,A)} n_H [\sigma_{(Z,A),(Z',A')} + \sigma_{(Z'',A''),(Z',A')}] vN_{(Z',A',z')} + [S_{(Z,A,z)} + S_{(Z'',A'',z'')}] - \frac{1}{\gamma\tau^*_{(Z,A)}} N_{(Z,A,z)} + \sum_{(Z''',A''')} \frac{1}{\gamma\tau^*_{(Z''',A''')}} N_{(Z''',A''',z''')} \tag{25}$$

Equation (25), when generalized, shows that by (1) redefining an effective partial fragmentation cross section as the sum over the set of all the short-lived parents plus the daughter nucleus, (2) redefining the source strength as the sum over the same set, and (3) summing over all gains through radioactive decays to either the short-lived parents or the daughter, then those nuclei which satisfy inequality (23) need not be explicitly treated.

How short-lived must a decay be in order for inequality (23) to hold? The answer is a function of the values of the parameters and constants within a model and should be determined self consistently. Most important is to know the size of the 1 σ -confidence region for the parameters n_H and τ because the values used in inequality (23) are not necessarily the best fit values. In particular, previous studies have found that only the product, $n_H\tau$, of the parameters (or equivalently the grammage x_o) can be well-determined. Hence if $\gamma \sim 2.4$ (see § II.(i)), and $\sigma \lesssim 950$ mb (see § II.d), while $x_o \sim 5$ gm/cm^2, and $\tau_{best} \sim 1.5 \times 10^7$y (Garcia-Munoz et al. 1977), then the inequality becomes

$$\tau_{*(Z'',A'')} << 1.6 \times 10^6 \text{ y } (\tau_{(Z'',A'',z'')}/\tau_{best}) \qquad (26a)$$

or

$$T_{\frac{1}{2}(Z'',A'')} << 1.1 \times 10^6 \text{ y } (\tau_{(Z'',A'',z'')}/\tau_{best}) \qquad (26b)$$

Thus in order to allow $\tau_{(Z'',Z'',z'')}$ to vary up to two orders of magnitude away from its best fit value, and at the same time keep the right hand side of the inequality at least an order of magnitude larger than the left hand side means (Z'',A'') should have a half-life less than 1100 y. Put another way, a long-lived nucleus can be defined as any β-active nucleus with a half-life, $T_{\frac{1}{2}}$, such that

$$T_{\frac{1}{2}} \geq 1100 \text{ y} \quad . \tag{27}$$

Applying the reduction procedures for electron capture isotopes and β-active nuclei yields the minimum number of nuclides to be explicitly treated. Sections II(b) - (i) give the quantitative values necessary to perform this reduction and propagate those that remain. A discussion of details is deferred until later; however, for a preview of the resulting simplified chart of the nuclides, see Fig. 2.

(b) Stripping Cross Section

As discussed above, the stripping cross section explicitly enters only in the treatment of electron capture isotopes. What is needed is the cross section for ionizing a hydrogenic atom that is in its ground state and is moving relativistically through the interstellar medium. The formula used by almost all cosmic ray researchers (cf. Reames 1974, Raisbeck 1974, but also Fowler et al. 1970) has been an expression due to Bohr (1948). However, as discussed in Appendix A, Bohr's formula is in error because it neglects ionizations via distant collisions (I thank Ray Hagstrom (Hagstrom 1977) for originally suggesting this possibility.)

As is also discussed in Appendix A, an improved approximation for low-Z media is the expression

$$\sigma_{strip} = \frac{4\pi a_o^2 \alpha^2}{Z_{CR}^2 \beta^2} (Z_{med}^2 + Z_{med}) \left\{ C_1 \left[\ln\left(\frac{(4\beta^2\gamma^2)}{C_2 Z_{CR}^2 \alpha^2}\right) - \beta^2 \right] \right\} \qquad (28)$$

where the factor in curly brackets isolates the deviations from the Bohr formula and where a_o is the Bohr radius,

α is the fine structure constant,

Z_{med} is the nuclear charge of the medium,

Z_{CR} is the nuclear charge of the cosmic ray,

and the constants C_1 and C_2 have the values 0.285 and 0.048, respectively. An expression for σ_{strip} that is virtually identical to Eq. (28) is given in Appendix B of Fowler et al. (1970). Their equation was given with little discussion, was without derivation, and was neither adopted nor discussed by other workers. The treatment given in Appendix A of this work was completed before I knew of the Fowler et al. formula.

Recall that in Eq. (1) all of the cross sections were expressed as per hydrogen atom, thus Eq. (28) needs to be averaged over the light constituents of the confinement volume. Assuming that the He abundance of the medium is as given in the Cameron (1973) compilation (He/H = 6.9%), the effective cross section per hydrogen atom is then given by

$$\sigma_{strip} = (4.53 \times 10^{-20}\ cm^2/\beta^2 Z_{CR}^2)\ [4.06 + .57\ \ln(\beta\gamma/Z_{CR}) - .285\ \beta^2] \quad (29)$$

Lastly note that the uncertainty of the interstellar He abundance, coupled with the approximation involved in deriving Eq. (28), means that the error in Eq. (29) is approximately 20%.

(c) Attachment Cross Section

As has been pointed out by Raisbeck and Yiou (1971), there are two distinct processes that can lead to electron attachment: radiative and non-radiative (which dominates at lower energies.) Further, because of the low density of the interstellar medium, attachments into excited states are always followed by electromagnetic cascades to the ground state. Thus, to obtain the effective cross section for attachment, one must both sum over the cross sections to capture into excited states and sum over the constituents of the medium.

(i) Radiative attachment

As the inverse to photoionization, radiative attachment is a two-body process in which an initially "free" electron becomes bound to a nucleus and an energy-conserving photon is emitted. In this context, the word free means that the orbital velocities of electrons in the medium are negligible when compared to the cosmic ray velocity. In the rest frame of the cosmic ray, the incident electrons then have a kinetic energy given by

$$Te = (m_e/m_u)T \quad (30)$$

where m_e is the electron rest mass, m_u is the mass of an atomic mass unit, and T is the kinetic energy per nucleon of the cosmic ray, as measured in the lab frame. Sunce T > 1 GeV, Eq. (30) shows both that the final binding energy is negligible compared to T_e and also that the relativistic theory of radiative attachment or photoionization is required. Using the principle of detailed balance one gets

$$\sigma_{RA} = \sigma_{PhI} \left[\frac{2(\hbar\omega)^2}{P_e E_e c} \right] \frac{1}{\beta_e} \tag{31}$$

where σ_{PhI} is the photoionization cross section per electron, $\hbar\omega$ is the energy of the emitted photon, and β_e, P_e, E_e are the velocity, momenta, and total energy of the "incident" electron. Note that the factor in brackets comes from the ratio of the densities of final states (including polarization degeneracy) while the remaining factor comes from the ratio of the relative velocities of the incident particles.

When Raisbeck and Yiou used Eq. (31), they substituted the photoionization cross section originally obtained by Sauter (1931) and given in Heitler (1954). However, as discussed in a review by Pratt, Ron, and Tseng (1973), the Sauter calculation is systematically higher than experimental data. In fact, deviations can range up to factors of 2 even for elements as light as aluminum. Much of this discrepancy stems from the fact that the electron wave function is significantly affected by the Coulomb field of the nucleus, even at energies much greater than the ionization potential. Although there does not exist a fully analytic expression for improving the Sauter form, Pratt et al.

have shown that a semi-empirical formula that combines the analytic expressions for two limiting cases does fit the data. Incorporating both their correction function and the Sauter formula into Eq. (31), and multiplying by Z_{med}, the number of "free" electrons per atom, gives the cross section per atom for attachment into the 1s state, namely

$$\sigma_{att,1s}^{rad} = \frac{3}{2} Z_{CR}^{5} Z_{med} \alpha^{4} \sigma_{T} \left[\frac{T_e^2}{(T_e + m_e c^2)^2 - m_e^2 c^4} \left(\frac{m_e c^2}{T_e}\right)^5 \right]$$

$$\times (\beta\gamma)^3 \left[\frac{4}{3} + \frac{\gamma(\gamma - 2)}{\gamma + 1} \left(1 - \frac{1}{2\beta\gamma^2} \ln\left(\frac{1 + \beta}{1 - \beta}\right)\right)\right] f_{cor} \quad . \tag{32}$$

The correction function f_{cor} is given by the equation

$$f_{corr} = a^{2\xi} \exp[-2(a/\beta) \cos^{-1}(a)]$$

$$\times \{1 + \pi a [N(\beta)/M(\beta)] + R(a)\} \tag{33}$$

where

$$\gamma = 1 + T_e/m_e c^2 = 1 + T/m_u c^2 \quad ,$$

$$\beta = (1 - 1/\gamma^2)^{\frac{1}{2}}$$

$$\sigma_T = 8\pi r_o^2/3 \quad \text{(the Thompson cross section)},$$

$$a = Z_{CR}\,\alpha \quad ,$$

$$\xi = -1 + (1-a^2)^{\frac{1}{2}} \quad ,$$

$$M(\beta) = 4/3 + \frac{\gamma(\gamma - 2)}{\gamma + 1}\left(1 - \frac{1}{2\beta\gamma^2}\ln\left(\frac{1 + \beta}{1 - \beta}\right)\right) .$$

$$N(\beta) = \frac{1}{\beta^3}\left[\frac{-4\gamma}{15} + \frac{34}{15} - \frac{63}{15}\frac{1}{\gamma} + \frac{25}{15}\frac{1}{\gamma^2} - \frac{8}{15}\frac{1}{\gamma^3}\right.$$

$$\left. - \frac{(\gamma - 2)\,(\gamma - 1)}{2\beta\gamma^3}\ln\left(\frac{1 + \beta}{1 - \beta}\right)\right] \quad , \quad \text{and}$$

$R(a) << 1$ and tabulated by Pratt et al.

The term $R(a)$ is small for all a; in fact for $Z_{CR} < 29$, $R(a) < 4 \times 10^{-4}$. Therefore, in this work $R(a)$ has been neglected. Also note that in the extreme relativistic limit Eq. (32) takes the form

$$\sigma_{att,ls}^{lim} = \frac{3}{2} Z_{CR}^5 Z_{med}\,\alpha^4\,\sigma_T\left(\frac{m_e c^2}{T_e}\right) f_{cor}^{lim} \tag{34}$$

with

$$f_{cor}^{lim} = a^{2\xi}\,\exp(-2a\,\cos^{-1}(a))\left\{1 - \frac{4}{15}\pi\,a\right\} \tag{35}$$

It is this slower decrease with energy that allows the radiative terms to eventually exceed the non-radiative terms.

For attachments into higher states, the results from Oppenheimer (1928) can be used. Oppenheimer studied the non-radiative process and showed that for $\alpha/\beta \ll 1$ only the higher s states provide significant contributions and that the ratio $(\sigma_n/\sigma_1) \approx n^{-3}$, where n is the principal quantum number. However, one can show that this n^{-3} "rule" holds for the radiative case also (cf. Bethe and Salpeter 1957). Therefore for a given constituent the radiative attachment cross section is given by

$$\sigma_{att}^{rad} \approx \sigma_{att,1s}^{rad} \sum_{n=1}^{\infty} n^{-3} = 1.202\ \sigma_{att,1s}^{rad}$$

and the limiting cross section becomes

$$\sigma_{att}^{lim} = 3.17 \times 10^{-33}\ Z_{CR}^{5}\ Z_{med}\ f_{cor}^{lim}/T \quad cm^2 \tag{36}$$

where T is in units of GeV/nucleon.

(ii) Non-radiative attachment

The non-radiative process is a quantum mechanical three-body problem involving the transfer of the electron from one nucleus to the other. Little work exists on the relativistic problem; in fact, there is even some disagreement about how to compute an accurate non-relativistic cross section (see Mott and Massey (1965, ch XIX).

The disagreement centers about whether a first Born approximation should neglect the (nucleus)-(incident particle) interaction. However, there is agreement that the Brinkman-Kramers relation (Brinkman and Kramers 1930), provides a reliable upper limit to the magnitude of the cross section and provides the asymptotically but non-relativistically correct scaling with energy and charge. Because it turns out that its contribution becomes negligible at relativistic energies (see § II.(iii)), it suffices to use this upper limit for comparison with the radiative term

The Brinkman-Kramers relation for attachment into the 1s state is given by

$$\sigma^{BK}_{att,1s} = (\pi a_o^2 2^{18}/5) Z_{CR}^5 Z_{med}^5 \, s^8 \qquad (37)$$

$$\times \left[s^2 + (Z_{CR} + Z_{med})^2\right]^{-5} \left[s^2 + (Z_{CR} - Z_{med})^2\right]^{-5}$$

where $s = \beta/\alpha = v/v_o$, a_o is the Bohr radius, and $v_o = e^2/\hbar$. The calculation pertains to a hydrogenic medium and requires z_{med}/s, $Z_{CR}/s < 1$. As discussed by Jackson and Schiff (1953) and Bohr (1948), one can think of the cross section as coming from an "overlap" between the momentum per nucleon of the incident particle and the momentum space wave function of the bound electron. On this basis, only the K shell electrons of a non-hydrogenic atom will have wave functions that extend to sufficiently high momenta. One K shell electron also partially screens the nuclear charge from the other, so

that the Z_{med} in Eq. (37) should not be the full nuclear charge for a non-hydrogenic medium. Thus, to obtain a more realistic limit for a non-relativistic velocity much greater than the electron's orbital velocity on either nucleus, Eq. (37) should be modified to

$$\sigma^{BK}_{att,1s} = r_K(\pi a_o^2 2^{18}/5) Z_{CR}^5 (Z_{med}-s_1)^5 \ \alpha^{12}/\beta^{12} \tag{38}$$

where r_K is the number of K shell electrons, and s_1 is the inner screening constant (0, for hydrogen medium; 0.3, otherwise , Slater 1930). As discussed above, for attachments into higher states, one can use the Oppenheimer n^{-3} "rule" so that the actual cross section satisfies the inequality

$$\sigma^{nrad}_{att} < 1.202 \ \sigma^{BK}_{att,1s} \tag{39}$$

After substituting for the constants and letting $r_K = 2$, inequality (39) becomes

$$\sigma^{nrad}_{att} < \left\{ \begin{array}{l} 2.53 \times 10^{-37}/\beta^{12} \\ 2.58 \times 10^{-39}/T^6 \\ 2.53 \times 10^{-37}/(\gamma^{10} \ \beta^{12}) \end{array} \right\} Z_{CR}^5 \ (Z_{med} - .3)^5 \ \text{cm}^2 \tag{40}$$

where T is in GeV/nucleon. The purpose of the three expressions in inequality (40) is to emphasize the dilemma in attempting even a qualitative extrapolation of the non-relativistic Brinkman-Kramers formula. The first form would hold if β were the correct variable in both the non-relativistic and the relativistic regimes. The second would hold if the relationship $T = 1/2\ m_u\ c^2\beta^2$ were first used in the non-relativistic form and then the resulting T^{-6} law extrapolated into the relativistic regime. The third would hold if momentum per nucleon were the relevant variable in both regimes and the relativistic increase in the density of final states were accounted for (since $\gamma \to 1$ for $\beta << 1$). Thus the choice of extrapolation can lead to a difference of almost 4 orders of magnitude at $\sim$ 1 GeV/nucleon. The preliminary analysis of recent attachment experiments by Raisbeck et al. (1977a) shows that the first form of inequality (40) is inconsistent with their data and that the middle form provides a satisfactory upper limit. Therefore, the kinetic energy extrapolation will be used in this work.

(iii) Magnitude of the attachment cross section

The ratio of the non-radiative to radiative formulae is a strong function of both the kinetic energy of the cosmic ray and the relative amount of high Z elements that are present in the medium. However, if the kinetic energy extrapolation law is used for the non-radiative case and if the relative iron abundance in the containment region is given by the Cameron (1973) table ($n_{Fe}/n_H = 2.6 \times 10^{-5}$), then a weighted sum over the constituents

of the medium shows that the non-radiative attachment process becomes negligible when compared to the radiative.

Recall that the attachment cross section of Eq. (1) was defined per hydrogen atom. Thus the effective attachment cross section is given by

$$\sigma_{att} = 1.202 \times \sigma^{rad}_{att,1s}(Z_{med} = 1) \left\{ \sum_{med} Z_{med} \left(n_{Z_{med}}/n_H\right) \right\} \tag{41}$$

$$= 1.38\ \sigma^{rad}_{att,1s}\ (Z_{med} = 1) \tag{42}$$

where the Cameron abundances were used to evaluate the term enclosed in brackets in Eq. (41).

As discussed in § II(a), the attachment cross section can be important in the propagation of electron capture isotopes. Thus in Table 1, a list is provided of the total effective attachment cross sections for those elements between lithium and nickel which have electron capture isotopes. The tabulation is for three energies (1, 3 and 5 GeV/nucleon and provides at each energy the value of the correction function (Eq. [33]). Although the cross sections in Table 1 are quite small relative to atomic dimensions, they are very comparable to, and often exceed, the characteristic size of partial fragmentation cross sections. It is this latter comparison that is most relevant for propagation.

Lastly, note that because σ_{att} is derived by detailed balance from a photoionization formula of high accuracy, it has a negligibly small uncertainty (i.e. less than 10%).

(d) Total Reaction Cross Section

The total reaction cross section represents the cross section for a "catastrophic" loss of the cosmic ray. That is, it is a sum over all cases in which an interaction caused either a change in the number of its nucleons or caused an inelastic energy loss that left it intact. (Recall that this work assumes that the inelastic-yet-intact events can be ignored.) In principle, values for the reaction cross section are required for each target species present in the interstellar medium.

The best set of data using a proton projectile appears to be that of Renberg et al. (1972), who obtained data at 4 different proton energies between 220 and 570 MeV and with 12 different targets. In addition, they tabulated existing data in the energy range from 10 MeV to 10 GeV. Their curves show that above 200 MeV the proton reaction cross section for targets other than hydrogen becomes nearly constant (i.e., variations are $\lesssim$ 5%). However, since some of the data are accurate to $\lesssim$ 2%, an alternative interpretation is that there are indications that each cross section reaches a maximum near 2 GeV and then decreases slowly at higher energies.

A common parameterization for such data has been the two parameter Bradt-Peters (1950) form of $\sigma_o\ (1 + A^{1/3} - b)^2$ (cf. Juliusson et al. 1975), where A is the atomic mass of the target. However, another fit, involving essentially no free parameters, is provided

by the theoretical calculations of Karol (1975). Working in the optical limit of Glauber theory, Karol derived an expression for the nucleus-nucleus reaction cross section in terms of the experimental parameters of the nuclear density distribution and the nucleon-nucleon cross sections. His calculation provides a natural explanation for both the limited variation of the cross section as a function of energy and the occurrence of a slight maximum near 2 GeV. The near constancy stems from the roughly logarithmic dependence upon the total nucleon-nucleon cross section. The maximum comes from the fact that the nucleon-nucleon cross section peaks near 2 GeV.

Karol's expressions are systematically higher than the Renberg et al. data by approximately 4%. More precisely, if the highest energy points of the ten targets (including compounds) that did not contain hydrogen are used, then

$$< \sigma_{Karol}/\sigma_{Renberg} > \equiv f_k = 1.037 \pm .009 \qquad (43)$$

where the error was computed as if the deviations from the mean were independent of target.

Table 2 provides a comparison between the experimental data of Renberg et al. and Karol's formulae (after dividing by Eq. (43). Also compared in the table is an even more phenomenological fit using the Bradt-Peters form. The input to the non-linear least squares fitting program consisted of the same independent points used to determine Eq. (43). The output consisted of the best values and the error matrix for the parameters σ_o and b. These quantities

are given in Table 3, and were used to derive the Bradt-Peters column in Table 2. It is quite clear that both the two-parameter Bradt-Peters form and the "renormalized" Karol results are in good agreement with the proton-nucleus data.

A further comparison of theory with experiment is provided by the data of Jaros (1975), who measured nucleus-nucleus reaction cross sections for light projectiles and targets. As in the case of proton-nucleus, Jaros' data are systematically lower than the Karol prediction, but this trend has less significance since the individual cross sections are only good to $\approx 5\%$. However, for consistency with Table 2, the comparison shown in Table 4 was made after Karol's formulae were also divided by Eq. (43). Although this table shows more scatter between theory and experiment than was shown in Table 2, Karol's version of Glauber theory is, again, in good agreement.

The data of Lindstrom et al. (1975a) allow an estimate of the importance of inelastic-yet-intact events and hence provide a test of the assumption that the cross section for such cases is small (see § I (a)). That is, since they measured the transmutation (or fragmentation) cross section for nucleus-nucleus reactions, any systematic difference from the Karol results would likely be from such events. For nucleus-proton collisions, their data compare closely with the Karol results. For nucleus-nucleus collisions their measurements are low by 8-18%. However, after this discrepancy is weighted by the relative abundance of the elements heavier than hydrogen, the approximation of Eq. (2) will remain appropriate.

Recall that in Eq. (1) the total reaction cross section was defined as the "effective" cross section per atom of interstellar hydrogen. Because the reaction cross section $\sim Z^{2/3}$, the only other relevant target material is interstellar helium with an abundance (relative to hydrogen)[1] of 0.07 (Cameron (1973)). The effective cross sections that result from the Karol formulae (divided by Eq. (43)) are given in Fig. 2. Note that for consistency with the off-diagonal terms (see § II(e)) a kinetic energy of 2.3 GeV/nucleon was assumed for the calculation.

For studies of the effects of random error, an uncorrelated error of 10% should be used. This figure comes mainly from the fact that to be consistent with assumption about the off-diagonal terms, the cross section would have to be treated as a constant, independent of energy. Additional contributions come from the variations in the results when either the parameters are varied or the composition of the interstellar medium is modified.

(e) Partial fragmentation cross sections

The partial fragmentation cross sections represent the inclusive cross section for producing a particular nucleus as the result of the fragmentation of a heavier parent nucleus. In principle, values for this cross section, as a function of energy, are required for each target species present in the interstellar medium. A valuable simplification is that at high energies ($\gtrsim$2 GeV/nucleon) the partial cross sections appear to reach asymptotic values (i.e., variations $\lesssim$10%)

[1] It is more common to use 0.1. However, for internal consistency the Cameron value was used.

and can be taken as approximately energy-independent (Lindstrom et al. 1975b; however, see also Raisbeck and Yiou 1975c).

Note the large number of cross sections that are required. Even after applying all of the reduction procedures of § II(a), there are 84 fully stripped isotopes with $3 \leq Z \leq 28$ (see Fig. 2). Because each of these isotopes is coupled to all higher isotopes, 3570 partial cross sections (constituting most of the off-diagonal elements of the modification matrix) are needed. As might be expected, only a limited number of these cross sections have been measured, and at very few energies, so that one must turn to phenomenology.

The most successful parameterizations of proton-nucleus data are the semi-empirical formulae of Silberberg and Tsao (1973a,b). For nuclei with $Z \leq 28$, they distinguish between two types of reactions--spallation and peripheral--and provide quite separate functional forms. These formulae were updated by Silberberg and Tsao (1977) to incorporate some of the systematics of recent experimental data and to correct errors in their earlier paper. Thus, if recent measurements are not available the appropriate semi-empirical formula provides the best estimate for the needed cross section.

Following Raisbeck and Yiou (1973) and Meneguzzi et al. (1975), a uniform error of 30% is assumed on all semi-empirical cross sections. This error assignment is also consistent with the standard deviation for $\sigma_{calc}/\sigma_{exp}$ found by Silberberg and Tsao in their original study.

Recall that the partial cross sections in the matrix M represent the production of both the "stable" isotope and any of its short-lived progenitors (see § II(a)). Experimental data represent a similar sum

and it is important to determine the number of "channels" over which a measurement has been summed. For example, secondaries with lifetimes $> 10^{-8}$ sec are individually measured by the direct projectile frame observations of Lindstrom et al. (1975b), while only secondaries with lifetimes ≥ 5 days are individually measured by the target frame, mass spectrometry observations of the Orsay group (Yiou et al. 1973, Raisbeck and Yiou 1975a, Raisbeck et al. 1975, and Perron 1976). Also, there are a few cases in which not all of the channels of a partial production cross section have been experimentally determined. For example, Raisbeck and Yiou (1975a) measured the cross section for producing ^{22}Na from protons on a Si target, but not for producting ^{22}F and ^{22}Ne. However, ^{22}Na decays to ^{22}Ne with a half-life of 2.6 years while ^{22}F decays to ^{22}Ne with a half-life of 4 sec, so that all three isotopes actually contribute to the "summed" partial cross section for producing ^{22}Ne (cf § II (a)).

With four exceptions, Table 5 provides a list of "summed" partial cross sections which have at least one channel measured in a recent experiment,[1] and were measured at energies greater than 2.1 GeV/nucleon. The errors were obtained by assuming the individual terms in the sum had independent, random errors. In cases such as the ^{22}Ne example given above, the semi-empirical formulae at a kinetic energy of

---

[1]Those labeled with a e were obtained by assuming semi-empirical predictions for Ni and Fe would deviate from experiment in the same way. Hence, the semi-empirical cross sections for production by a proton with 2.3 GeV on Fe were scaled by the ratio $\sigma_{exp,Ni}/\sigma_{calc,Ni}$. As with other semi-empirical cross sections, a 30% error was assumed.

2.3 GeV/nucleon[1] were used for the unmeasured contributors. The error for the semi-empirical cross sections was set at the fraction necessary to produce a 30% error if no terms had been determined experimentally. For example, for ^{22}Ne a 40% error in the ^{22}F + ^{22}Ne portion is combined with the 9% experimental error on ^{22}Na to obtain the 14% error shown in Table 5.

All that remains is to incorporate the effects of the constituents of the interstellar medium heavier than hydrogen. However, there are very limited data for relativistic alpha particles on complex nuclei (Raisbeck and Yiou 1975b) and no data for nuclei incident on helium targets. Raisbeck and Yiou found that the average of the high energy α-induced to proton-induced cross sections was 1.74 ± 0.23 and that the ratio for light targets was approximately independent of energy. Some of the cross section ratios for the production of fragments much lighter than the parent nucleus did show significant variations with energy. However, as pointed out by Raisbeck and Yiou, such modes make negligible contributions to the overall abundance of a fragment. Thus, the above ratio can be taken as "universal". With this assumption, the effective cross section per hydrogen atom is then given by the equation

$$\sigma = \sigma_p[1 + (\sigma_\alpha/\sigma_p)\ (n_{He}/n_H)] \qquad (44)$$

---

[1]The semi-empirical formulae become energy-independent for kinetic energies > 2.3 GeV/nucleon.

where $\sigma_p(\sigma_\alpha)$ denotes proton (α)-induced fragmentations and n_{He}/n_H is the relative abundance of helium in the interstellar medium. Thus, since $\sigma_\alpha/\sigma_p = 1.74 \pm 0.23$ and $n_{Ne}/n_H = 0.07 \pm 0.03$,[1] Eq. (44) becomes

$$\sigma = 1.12\ \sigma_p[1 \pm 0.05] \tag{45}$$

Note that the extra 5% error in Eq. (45) makes no difference when combined with the 30% error on all semi-empirical cross sections. However, the extra error does increase the errors on the effective cross sections above those given in Table 5.

A table of all of the 3570 partial fragmentation cross sections would be unwieldy and has not been included. A smaller table of "weighted" cross sections has been included as a part of Table 8. For details of the table's construction see § III.

(f) Half-lives

As shown in § II(a), separate entries in the column vectors are required for isotopes that, as cosmic rays have β-decay half-lives greater than 1100 years. Also, the half-life required is that for a fast nucleus having at most one K-shell electron and not that for a neutral atom with a full complement of orbital electrons. In principle, this difference in "environment" for the nucleus leads to a difference in its decay rate. The discussion below is directed towards isolating

---

[1]The error assignment for n_{He}/n_N reflects the decision that the "canonical" value of 10% by number must lie within the 1-σ limits of the Cameron (1973) value. The error does not stem from a study of experimental measurements.

those effects which can cause the decay rate of a neutral atom to differ by more than approximately five per cent from that of the stripped nucleus.

As discussed by Bahcall (1963), the decay of an unstable nuclide in the lab should be described in terms of the atomic states involved. Hence, if H_β represents the Hamiltonian for beta-decay, the decay rate takes the symbolic form ($\hbar = c = 1$)

$$\lambda = 2\pi \mid \langle f \mid H_\beta \mid i \rangle \mid^2 \delta(E_f - E_i) \tag{46}$$

where the full atomic energies are included in E_i and E_f, and $|i>$ and $|f>$ represent the initial and final states. More explicitly, $|i> = |G;k>$ and $|f> = |A'; e^{\pm}; \nu; k>$ where $|G>$ is the state vector for the atom in its ground state, $|A'>$ represents any of the final states of the daughter ion (including continuum states for some electrons), $|k>$, $|k'>$ denote the initial and final nuclear variables, $|e^{\pm}>$ denotes the positron (electron) variables, and $|\nu>$ denotes the neutrino variable. The atomic environment enters in both the description of the states $|e^{\pm}>$, and in the energy conserving delta-function, as well as in the states $|G>$ and $|A'>$.

The description of the continuum state $|e^{\pm}>$ enters via the Fermi function $F_{\pm}(Z,W)$ and the shape function $S_n(W,Z)$ (applicable in forbidden decays). To determine the impact on the half-life, an estimate is required of the effect the screening by orbital electrons has on these functions, when Eq. (46) is integrated over the entire spectrum of electron energies. For allowed decays a comparison of screened and unscreened results is provided by Behrens and Jänecke (1969)

and Gove and Martin (1971). Moreover, Good (1954) showed that the effect of screening on a forbidden spectrum is comparable to the effect on an allowed spectrum.

The graphs of Behrens and Jänecke show that for $Z \leq 40$, the effect of screening on the integrated statistical factor for electron emission is less than 2 per cent, regardless of endpoint energy. For positron emission their curves show that the effect decreases rapidly with increasing endpoint energy. They show that for $Z \leq 28$ and endpoint energies ≥ 800 keV and for $Z \leq 19$ and energies ≥ 450 keV, screening has less than a 2 per cent effect on the statistical factor for positrons. In keeping with Good's finding, it will be assumed that if screening makes less than a 2 per cent change in the rate for an allowed decay that has the same Z and endpoint energy as a forbidden decay, then its effect on the forbidden decay will be less than the "threshold" of ≈ 5 per cent. As discussed above, this limited dependence means that the effect of screening can be neglected in this work.

The dependence of the beta-decay on the remaining "environment" factors is even smaller. As discussed by Bahcall (1963), the argument of the energy-conserving delta function can be written in the form

$$E_i - E_f = (E_i^{o} - E_f^{o}) + E(G') - E(A')$$

where $E_i^{o} - E_f^{o}$ is the usual atomic mass difference and $E(G')$, $E(A')$ are the atomic binding energies of the ground state $|G'>$ and the arbitrary state $|A'>$, respectively. By "expanding" the delta-function in terms of the difference $E_i^{o} - E_f^{o}$ and taking advantage of closure

via the sum over final states, he showed that there is a slight decrease in the decay rate because of the overlap with a large number of final states. He found that if $\bar{E}_{ex}$ denotes the average excitation of the final atom, then the fractional decrease in the total decay rate, $\Delta\lambda/\lambda$, is given by

$$\Delta\lambda/\lambda \sim \bar{E}_{ex}/E_{max} \quad , \tag{47}$$

where E_{max} is the maximum kinetic energy (or endpoint energy) for the decay. His calculation dealt only with allowed decays. However, since the additional energy dependence of the shape factors enters only via the coefficient that multiplies $(\bar{E}_{ex}/E_{max})$, it also can be used to determine the order of magnitude of the decrease for forbidden decays. In addition, he obtained the estimates

$$\bar{E}_{ex} = -\tfrac{1}{2} \left\{ \begin{array}{ll} 49Z^{1/3} \text{ eV} , & \text{if } Z < 10 \\ 46Z^{2/5} \text{ eV} , & \text{if } Z > 10 \end{array} \right\} \tag{48}$$

with a smooth joining of the two forms at $Z = 10$.

A further environmental effect for electron emission (Bahcall) 1963) involves an exchange mechanism whereby the initially present is electron is "flipped into the continuum state, making room for the creation of a 1s' electron by the decaying nucleus." Bahcall found that this mechanism was competitive with the shift given by estimate (47). However, because of the higher powers of the nuclear radius

involved in a forbidden decay, this mechanism contributes very little to the dependence of a forbidden decay rate on the presence of atomic electrons.

Table 6 provides a compilation of the endpoint energies (in keV) and decay modes of the isotopes with $Z \leq 28$ that have laboratory half-lives greater than 1100 years. Equations (47) and (48), as well as the graphs of Behrens and Jänecke, show that the right hand side of Eq. (47) never exceeds 6×10^{-4} and that only the β_+ - decay of ^{36}Cl fails the 2 per cent criterion for screening. The β_+ decay of ^{36}Cl has such a small branching ratio that the removal of the effect of screening will still have no effect on the total decay rate. Thus it suffices, for this work, to treat all of the decay rates for electron and positron emission, as if they were independent of their atomic environment. As will be seen below, no such conclusion is possible for electron capture.

(1) Isotopes with electron capture branches

For an isotope with a long laboratory half-life that decays by both beta emission and electron capture, the half-life as a cosmic ray increases because of the suppression of its electron capture branch. To verify this claim, let τ_L be the mean life for a neutral atom in the laboratory and let r_{EC} be its branching ratio (in the lab) for electron capture. As discussed above, the beta-decay portion of the lab decay rate is, to a very good approximation, independent of the presence of its atomic electrons so that the mean life for a cosmic ray to beta-decay, $\tau_{CR,\pm}$, is just

$$\tau_{CR,\pm} = \tau_L / (1 - r_{EC}). \tag{49}$$

However, the decay rate via electron capture depends upon having and keeping an electron attached. Thus, let τ_{strip} ($\equiv (n_H \sigma_{strip} v)^{-1}$) be the mean time between stripping collisions. If τ_L is so large that $\tau_{strip} << (\tau_L / r_{EC})$, then the stripping rate will be faster than the decay rate via electron capture. But under these circumstances (essentially the clock isotope criterion of § II(a)), the effective mean life for an electron capture by an unstable cosmic ray is approximated by (Yiou and Raisbeck 1970)

$$\tau_{CR,EC} \simeq 2 \, (\tau_L / r_{EC})(\sigma_{strip} / \sigma_{att}) \quad . \tag{50}$$

Since Eq. (29) and either Eq. (42) or Table 1 show that at energies $\gtrsim$ 1 GeV/nucleon the ratio $\sigma_{strip}/\sigma_{att}$ is $\gtrsim 10^3$ for the isotopes of interest in this work, Eq. (50) shows that the electron capture branch will be completely suppressed. Thus, the mean life as a cosmic ray becomes

$$\tau_{CR} = \tau_{CR,\pm} = \tau_L / (1 - r_{EC}) \quad . \tag{51}$$

As shown in Table 6, this suppression increases the half-lives of ^{26}Al [1], ^{36}Cl, and ^{40}K.

---

[1] Note that the first excited state of ^{26}Al only beta decays. Thus implicit in using the lifetime of the ^{26}Al ground state is the assumption that the fraction spalled into excited states is negligible or, equivalently, that its production cross section is only for interactions that produce ^{26}Al in the ground state (cf. Raisbeck et al. 1977b).

Even if its laboratory half-life is short, there is still a possibility for an isotope to have a long half-life as a cosmic ray. This chance arises when an isotope decays via electron capture but also has a Q value large enough to permit beta emission. Based on the 1977 Atomic Mass Evaluation (Wapstra and Bos 1977), the isotopes ^{54}Mn, ^{56}Ni, and ^{59}Ni are potential positron emitters, while ^{54}Mn is also a potential electron emitter. However, ^{59}Ni can be omitted because of the combination of its long lab half-life, $(8 \pm 1) \times 10^4$ y, and the recently determined branching ratio for positrons of 1.5×10^{-7} (Berenyi et al. 1976). Figure 1 gives level schemes for those branches of ^{54}Mn and ^{56}Ni that would involve beta emission. Note that for both nuclei the non-electron capture decays are so forbidden that they have not been observed in the lab.

As shown by Cassé (1973a, b), if both ^{54}Mn and ^{56}Ni are stripped of their atomic electrons, the relevant transitions for each are the 3^+ transitions[1] (also called unique second-order forbidden) which are indicated by the dotted lines in Fig. 1. He showed that in spite of its requiring only a change of 2 units of spin, the 2^+ transition had a negligibly small decay rate because of its very small endpoint energy. In addition, he showed that the two 4^+ and 5^+ transitions have negligible probability due to the very large change of spin and being, as a result, highly forbidden.

---

[1]Transitions are categorized by the difference in the nuclear spins and parities of the initial and final states. In this work these changes are written in the short-hand form ΔI^{π}, where ΔI denotes the spin change and π denotes the product of the initial and final parities.

Cassé also attempted to determine the half-lives for the remaining transitions by analyzing the variations of the log (ft) values of other 3^+ decays. In fact, he claimed somewhat accurate half-life estimates are possible, a point considered and rejected in Appendix B (cf. Raisbeck et al. 1973). The study of the well-determined second-order forbidden transitions given in Appendix B shows that there is too much dispersion in both the log $(f_0 t)$ and log $(f_2 t)$ values to provide a predictive capability. Instead one must hope that the dispersion in log (ft) values of such cases brackets the range of values for ^{54}Mn and ^{56}Ni. Table 6 shows the deduced ranges using this assumption.

Of course even as cosmic rays, ^{54}Mn and ^{56}Ni can still decay by electron capture if an electron has been attached. In fact, both are spallation isotopes (see § II(a)), so that the rate limiting step in their decay by electron capture is the atomic process of picking up an electron from the medium. That means the effective lifetime for decay by electron capture, $\tau_{EC,*}$, is given by the expression

$$\tau_{EC,*} = (n_H \sigma_{att} v)^{-1} = 2.1 \times 10^7 / (n_H \sigma_{50} \beta) \quad y \qquad (52)$$

where σ_{50} gives σ_{att} in units of 50 mb and n_H is in cm^{-3}. Since σ_{att} is a rapidly-decreasing function of energy, Eq. (52) shows it is quite possible to have the forbidden β-decay rate comparable to or even much larger than the effective rate via electron capture. Thus, a complete treatment of the propagation of ^{54}Mn and ^{56}Ni must include the effects of both forbidden β-decay and electron capture.

As discussed in § II(a), if an electron-capture isotope has a half-life that is too long to satisfy the spallation criterion then both the one-electron and fully-stripped cases must be included. Using Eq. (29) for σ_{strip}, this criterion is given quantitatively by the expression

$$\gamma\tau_{EC} << \frac{9.33 \times 10^3 (Z_{CR}/20)^2 \beta}{n_H(cm^{-3}) \, [2.35 + .571n(\beta\gamma/(Z_{CR}/20)) - .285 \beta^2]} \quad y \; . \qquad (53)$$

Those isotopes that fail to meet this criterion are called "clock" isotopes. Thus, this category includes ^{41}Ca, ^{44}Ti, ^{53}Mn, and ^{59}Ni (although ^{44}Ti needs to be included only when the density n_H is high or γ is large.) As in the cases above, the lifetimes of these nuclei will differ from the laboratory measurements. A first approximation for the life of the state with one orbital electron would be to merely double the lab half-life (because there is only 1 K-shell electron). However, as discussed in detail in Appendix C, there are two smaller effects. First, the decay rate is reduced by $\approx 10\%$ because there are no captures from the higher shells; and second, the rate is increased by $\approx 4\%$ because the nucleus is unscreened. The resulting half-lives are shown in Table 6.

(2) Other long-lived isotopes

For the four isotopes in Table 6 that have not already been mentioned, the cosmic-ray half-life is essentially unchanged from the laboratory half-life.

(g) The Isotope Fractions at the Source

As discussed in § I(b), the isotope fractions at the source, the non-zero components of the ν matrix, are not as fundamental an input as the quantities described in the earlier sections. In fact, once high energy observations can resolve isotopes, the ν array will be one of the basic findings of any propagation analysis. Until then, some assumption must be made. The assumption made in preparing Table 8 (see § III) was that the isotope fractions at the source are identical with those given by the Cameron (1973) compilation of the "universal" abundances. Explicit values of these fractions are provided in line 3 of Fig. 2.

Note that the choice of Cameron "fractions" carries with it the "hidden assumption" that the mean time between nucleosynthesis and acceleration (cf. Cassé and Soutoul 1975) is so long that all unstable species have negligible abundances at the time of acceleration. However, note also that without having a detailed model for the origin of at least all of the nuclides in Fig. 2, it is quite hard to relax this assumption of "universality".

(h) The Abundances at the Top of the Atmosphere

The abundances at the top of the atmosphere for all elements between Li and Ni, that is, the components of the $\underset{\sim}{N}$ column vector, constitute the final input quantity. The "best set" of such abuncances seems to be the compilation by Silberberg et al. (1976), whose Table 6 has been reproduced in Table 7 of this work. Note that the table provides relative abundances and errors for rigidities $R > 4$ GV.

III. Discussion

Using the input quantities from § II, the matrices and column vectors of § I can be constructed.

(a) Final list of the nuclides

The reduction procedure of § II(a), coupled with the parameters from § II(b)-(f), yields the minimum number of nuclides that must be explicitly propagated. The resulting simplified chart for those nuclides having atomic numbers between 3 and 28 is shown in Fig. 2. Note that for an unstable nucleus, line 1 gives the mode(s) of decay for the nucleus when it has at most one K-shell electron. The notation "a&EC" denotes the sequence electron attachment followed by electron capture. As noted earlier, "spallation" isotopes decay by this mode with a rate governed not by the laboratory half-life, but by the magnitude of the attachment cross section. The notation "a/EC" in line 1 denotes the sequence electron attachment followed more often by electron stripping but sometimes by electron capture. In these cases the half-life for the nucleus with one electron attached ($T_{\frac{1}{2},EC}$) is given in parentheses. As discussed earlier, "clock" isotopes decay by such a sequence. Note also that, as in the case of ^{60}Fe, short-lived intermediate links in a decay chain do not have to be explicitly propagated. Lastly, line 2 of the figure gives the total effective reaction cross section per hydrogen atom. As discussed in § II(d), these cross sections include an estimate of the contributions from interstellar helium and were calculated using a slight renormalization of Karol's analytic version of the Glauber formalism.

(b) The elemental modification matrix

In addition to its dependences on many of the quantities discussed in § II, the modification matrix is also a function of the parameters n_H and $\tau_{(Z,A,z)}$. In a quantitative propagation calculation, the values of these parameters are determined by testing the hypothesis that the source abundances of Li, Be, and B are zero. That is, values are determined that minimize the differences between the computed abundances at the top of the atmosphere and the actual abundances of Li, Be, and B. Such a study is beyond the scope of the present work. However, as shown below, some of the algebraic manipulations necessary to such a study also enter into the calculations of the elemental modification matrix.

As discussed earlier, the entire modification matrix would make a lengthy table in which most of the entries would not be based on recent experimental data. A more useful matrix is the "weighted", or elemental modification matrix, $\mathscr{M}$, which acts on $v\underset{\sim}{N}$ instead of the expression $v\varepsilon\underset{\sim}{N}$. To derive $\mathscr{M}$, first multiply Eq. (10) by M^{-1} and sum the resulting equation over all the isotopes belonging to the K-th element. Then, after Eq. (4a) is used to eliminate ε, the propagation equation becomes

$$v\underset{\sim}{N} + \mathscr{M}^{-1}\,\underset{\sim}{S} = 0 \tag{54}$$

where $\mathscr{M}^{-1}$ is given by the expression

$$\mathcal{M}_{KL}^{-1} = \sum_{i=i_1(K)}^{i_n(K)} M_{ij}^{-1} \nu_{jL} \qquad (55)$$

and where $i_1(K)$ denotes the first isotope belonging to the element in the K-th row of $\mathcal{M}^{-1}$ and $i_n(K)$ denotes the last isotope. Note two points about $\mathcal{M}$. First, as shown in Eq. (55), the collapse from isotope to element was done by weighting M^{-1} with the assumed isotope fractions at the source. Secondly, multiplying Eq. (54) by $\mathcal{M}$ gives the equation

$$\underset{\sim}{S} = -\mathcal{M}\, \nu \underset{\sim}{N} \quad , \qquad (56)$$

in which $\underset{\sim}{S}$ is completely specified in terms of the input quantities and the parameters.

Because so many of the terms of M and $\mathcal{M}$ have the form of a product of a cross section and the parameter n_H, it is more convenient for display purposes to give the matrices in the units of a cross section. Thus, Table 8 gives the value of $\mathcal{M}/n_H$ for the elements between Li and Ni. Note first that before the collapse of the larger matrix, the lifetimes were taken from Table 6, the kinetic energy was assumed to be 2.3 GeV/nucleon, the leakage time, τ, was assumed to be species-independent with a value of 1.5×10^7y, and n_H was given the value 0.2 cm^{-3}. The values for τ and n_H are taken from the lower energy study of Garcia-Munoz et al. (1977) but should be reasonable values at the higher energies of this work. Secondly, note that from the definitions of the F and D matrices (cf. § I(a)), if n_H is 0.2 cm^{-3},

then a half-life of 10^6y corresponds to an effective cross section of 1100 mb, while a leakage time of 1.5×10^7y corresponds to an effective cross section of 368 mb. Lastly, note that the errors shown just below and to the right of each term in $\mathcal{M}/n_H$ were obtained by the procedures discussed in Appendix D.

(c) The impact of the corrections and improvements

The major emphasis of this work has been to critically investigate the quantities that constitute the input to a quantitative propagation calculation. Less importance has been placed on the extent to which any corrections or improvements in the input will cause a change in the output. The reasons for this emphasis are two-fold. First, by emphasizing the nuclear and atomic physics that govern the composition of cosmic rays, this work is more fundamental and therefore less model-dependent. Secondly, because the well-determined output quantities tend to be insensitive to the net effect of the changes found in § II, while those that are sensitive are rather poorly determined, it turns out that few of the corrections will have an <u>immediate</u> quantitative impact.

This limited impact is very evident for the (well-determined) quantity $n_H\tau$. In this case the addition of the effects of interstellar helium to the off-diagonal terms of M will tend to lessen the changes in $(n_H\tau)$ that arise from adopting the cross sections given in Fig. 2. To illustrate this point, recall that the grammage, or equivalently $n_H\tau$, is most dependent on the L/M ratio, i.e. on the experimental quantity ([Li] + [Be] + [B])/([C] + [O]) where the bracket enclosing

each symbol denotes that element's abundance at the top of the atmosphere. Note also that the term $(1/\gamma\ \tau_d)[^{10}Be]$ cancels out if all the propagation equations for the isotopes of Li, Be, and B are added together. Thus, the equation for ([Li] + [Be] + [B]) can be written in the approximate form

$$\left(\frac{1}{v\tau} + n_H < \sigma_L >\right)\ ([Li] + [Be] + [B]) = n_H <\sigma_{LM}> ([C] + [O]) \qquad (57)$$

where $< \sigma_L >$ is an average reaction cross section for the isotopes of Li, Be, and B, and $< \sigma_{LM} >$ is an average partial cross section for producing the same isotopes from the isotopes of C and O. It follows from Eq. (57) that the constraint of producing a given L/M ratio as the input cross sections are varied can be translated into an equation governing the fractional change in $n_H \tau$. This equation is

$$\frac{\delta(n_H\tau)}{n_H\tau} = n_H\ \tau\ v < \sigma_L >\ r_L - (1 + n_H\tau\ v < \sigma_L >)\ r_{LM} \qquad (58)$$

where r_L is the fractional increase in $< \sigma_L >$ and r_{LM} is the fractional increase in $< \sigma_{LM} >$. As shown in Eq. (45), r_{LM} has the value 0.12. Since the difference between the cross sections given in Fig. 2 and the cross sections obtained by using the Bradt-Peters formula with the parameters of Table 3 is approximately 30%, $r_L \approx 0.30$. An estimate of $< \sigma_L >$ can be obtained by averaging, with uniform weights, the cross sections obtained with the Brad-Peters form. The result is

that $<\sigma_L> \approx 185$ mb. Thus at a kinetic energy of 2.3 GeV/nucleon and if $n_H \tau = 3$ My cm^{-3}, Eq. (58) shows that $n_H \tau$ will decrease by approximately 3%, even if the diagonal terms increase by 30% and the off-diagonal terms increase by 12%.

In the case of the attachment cross sections, the limited impact arises because the corrections further reduced the importance of the inclusion of a "spallation" coupling between a fully stripped isotope capable of decaying by electron capture and its daughter. Even the lengthened estimates of the lifetimes of several long-lived species do not dramatically increase the ability of those species to compete with the ^{10}Be clock.

The greatest change brought about by this work is to the effective life for those electron capture isotopes that are clock isotopes. Recall that for these isotopes the effective life for the fully stripped state depends on the term $(\sigma_{strip}/\sigma_{att})\ \tau_{EC}$, where τ_{EC} is the lifetime with one K-shell electron. Thus, since the corrections to σ_{strip} were approximately 60% while the corrections to σ_{att} were approximately a factor of two, both the ratio $(\sigma_{strip}/\sigma_{att})$ and the effective life will change by approximately a factor of 3.

Unfortunately, this large increase also has limited practical consequences. In the cases of ^{59}Ni, ^{41}Ca, and ^{53}Mn, the limitation stems from their already long lifetimes with one K-shell electron; while for ^{44}Ti, it arises from the requirement that it be a clock isotope. At high energies, the ratio $(\sigma_{strip}/\sigma_{att})$ is $\geq 10^4$ for these isotopes, while the lifetimes of the one-electron species of ^{59}Ni, ^{41}Ca, and ^{53}Mn are 1.7×10^5y, 2.2×10^5y, and 7.7×10^6y (see Table 6).

Thus, their effective lives are $\geq 10^9$y and any increase merely worsens the unfavorable comparison with a leakage time of the order 10^7y. Because the one-electron lifetime of ^{44}Ti is 100y , at high energies its effective life would be $\geq 10^6$y, if it were a clock isotope, i.e. if

$$\gamma\tau_{EC} \gtrsim (n_H \sigma_{strip} v)^{-1} \tag{59}$$

For a kinetic energy of 2.3 GeV/nucleon, Eq. (59) corresponds to the requirement that

$$n_H \geq 7.9 \text{ cm}^{-3} \tag{60}$$

The restriction of n_H to rather high values shows that ^{44}Ti is generally a spallation isotope and hence less dramatically affected by the changes of § II.

CONCLUSIONS

In contrast to most other studies relevant to the propagation of cosmic rays, in this study the major emphasis has been on developing the proper set of formulae for the atomic and nuclear processes that govern the composition. As a result, several calculations in relativistic atomic physics were required. These ranged from developing a better cross section for stripping an orbital electron to incorporating the change in the beta decay rate due to the fact that a cosmic ray nucleus is unscreened. The nuclear physics calculations ranged from computing reaction cross sections within the Glauber formalism of Karol to investigating the systematics of unique second-order forbidden beta decays. As was shown in § II,

this critical review of the input quantities for the "leaky box" model led to the detection of several errors in the standard values. These errors and their corrections are listed below:

(1) Deviations of approximately a factor of two were found between the standard (Bohr) cross sections for stripping and a more reliable estimate (also obtained by Fowler et al. 1970) that properly included distant collisions (see § II(b)).

(2) The correction function from high energy photoionization was properly introduced into the standard (Raisbeck and Yiou 1971) cross section for radiative attachment (see § II(c)).

(3) Because the half-life of a fast nucleus with at most one K-shell electron differs from the half-life of a neutral atom, several standard (laboratory-based) values had to be corrected. These corrections ranged from approximately a factor of 2 increase in the lifetimes of the one-electron states of clock isotopes to slight increases due to the suppression of electron capture branches (see § II(f)).

In addition to the above corrections, several improvements were presented. These advances are given below:

(1) For the reaction cross section, the Glauber formalism of Karol was introduced both as a means of reliably incorporating the effects of interstellar helium and as a less phenomenological method of parameterizing the data (see § II(d)).

(2) The effects of interstellar helium were also included for the first time in the partial production cross sections (see § II(e)).

(3) For all input quantities except the matrix ν, error estimates were given.

(4) A more complete analysis of unique second-forbidden beta decays with well-determined parameters was given. In contrast to the findings of an earlier study by Cassé, no predictive capability was discovered (see § II(f)) and Appendix B).

All of the error corrections and improvements were presented within the context of a matrix formalism for the propagation of relativistic cosmic rays within a "leaky box". In addition, it was shown that once the assumption of species-independent leakage was introduced, the formalism was essentially identical with the standard exponential path length formalism (see § I(c)).

I would like to acknowledge useful discussions with J. Stevenson, Dick Gordon, H. J. Crawford, P. J. Lindstrom, and Ray Hagstrom. In addition, I would like to thank P. B. Price and R. Cowsik for their patience and understanding during the lengthy gestation period for this study. This work was supported partially by Division of Nuclear Science, U.S. Department of Energy, and NASA Grant NAS-9-29603.

REFERENCES

Ajzenberg-Selove, F. and Lauritsen, T. 1974, Nucl. Phys. A227, 1.

Auble, R. L. 1977, Nucl. Data Sheets, 20, 253.

Bahcall, John N. 1963, Phys. Rev., 129, 2683.

Behrens, H. and Buhring, W. 1971, Nucl. Phys., A162, 111.

Behrens, H. and Janecke, J. 1969, Numerical Tables for Beta-Decay and Electron Capture, Landolt-Bornstein New Series-I/4, ed. H. Schopper (New York:Springer-Verlag).

Berenyi, D., Hock, G., Menes, A., Szekely, G., Ujhelyi, Cs., Zon, B. A. 1976, Nucl. Phys., A256, 87.

Bethe, H. A. and Salpeter, E. E. 1957, Quantum Mechanics of One- and Two-Electron Atoms (Berlin:Springer-Verlag).

Bjorken, J. D. and Drell, S. D. 1964, Relativistic Quantum Mechanics (San Francisco:McGraw-Hill), 52.

Bohr, N. 1948, Kgl. Danske Videnskab, Selskab. Mat.-fys. Medd., 18, No. 8.

Bradt, H. L. and Peters, B. 1950, Phys. Rev., 77, 54.

Brinkman, H. C. and Kramers, H. A. 1930, Proc. Acad. Sci., Amsterdam, 33, 973.

Bugg, D. V., Salter, D. C., Stafford, G. H., George, R. F., Riley, K. F., Tapper, R. J. 1966, Phys. Rev., 146, 980.

Cameron, A. G. W. 1973, Space Sci. Rev., 15, 121.

Cassé, M. 1973a, Ap. J., 180, 623.

_____. 1973b, Proc. 13th Int. Cosmic Ray Conf. (Denver), 1, 546.

Cassé, M. and Soutoul, A. 1975, Ap. J., 200, L75.

Cowsik, R., Pal, Y., Tandon, S. N., and Verma, R. P. 1967, Phys. Rev., 158, 1238.

Cowsik, R. and Wilson, L. W. 1973, Proc. 13th Int. Cosmic Ray. Conf. (Denver), 1, 500.

_____, 1975, Proc. 14th Int. Cosmic Ray Conf. (Munich), 2, 659.

de Jager, C. W., de Vries, H., and de Vries, C. 1974, Atomic Data and Nucl. Data Tables, 14, 479.

Dmitriev, I. S., Zhileikin, Ya. M., and Nikolayev, V. S. 1966, Soviet Phys.--JETP, 22, 352.

Drouin, J. R. S. and Yaffe, L. 1962, Canad. J. Chem., 40, 833.

Emery, J. F., Reynolds, S. A., Wyatt, E. I., Gleason, G. I. 1972, Nucl. Sci. and Eng., 48, 319.

Endt, P. M. and Van Der Leun, C. 1973, Nucl. Phys., A214, 1.

Fichtel, C. E. and Reames, D. V. 1966, Phys. Rev., 149, 995.

Fowler, P. H., Clapham, V. M., Cowen, V. G., Kidd, J. M., Moses, R. T. 1970, Proc. Roy. Soc., A318, 1.

Garcia-Munoz, M., Mason, G. M., and Simpson, J. A. 1977, Proc. 15th Int. Cosmic Ray Conf. (Plovdiv), 1, 224.

Ginzburg, V. L. and Syrovatskii, S. I. 1964, The Origin of Cosmic Rays, New York, Pergamon Press.

Gloeckler, G. and Jokipii, J. R. 1969, Phys. Rev. Lett., 22, 1448.

Good, R. H., Jr. 1954, Phys. Rev., 94, 931.

Gove, N. B. and Martin, M. J. 1971, Nucl. Data Tables, 10, 206.

Greiner, D. E., Lindstrom, P. J., Heckman, H. H., Cork, B., Bieser, F. S. 1975, Phys. Rev. Lett., 35, 152.

Hagen, F. A., Fisher, A. J., and Ormes, J. F. 1977, Ap. J., 212, 262.

Hagstrom, R. 1977, Private communication.

Heitler, W. 1954, The Quantum Theory of Radiation, 3d ed. (Oxford: Clarendon Press).

Heckman, H. H., Greiner, D. E., Lindstrom, P. J., Bieser, F. S. 1972, Phys. Rev. Lett., 28, 926.

Honda, M. and Imamura, M. 1971, Phys. Rev., C4, 1182.

Huang, K. N., Aoyagi, M., Chen, M. H., Crasemann, B. 1976, At. & Nucl. Data Tables, 18, 243.

Jackson, J. D. and Schiff, H. 1953, Phys. Rev., 89, 359.

Jaros, J. A. 1975, Lawrence Berkeley Laboratory report LBL-3849.

Juliusson, E., Cesarsky, C. J., Meneguzzi, M., Cassé, M. 1975, Proc. 14th Int. Cosmic Ray Conf. (Munich), 2, 653.

Karol, P. J. 1975, Phys. Rev. C11, 1203.

Kim, H. J. 1975, Nucl. Data Sheets, 16, 317.

Konopinski, E. J. and Rose, M. E. 1965, Alpha- Beta- and Gamma-Ray Spectroscopy, ed. K. Siegbahn (New York:American Elsevier Publishing), 2, 1360.

Lindstrom, P. J., Greiner, D. E., Heckman, H. H., Cork, B., and Bieser, F. S. 1975a, Proc. 14th Int. Cosmic Ray Conf. (Munich), 7, 2315.

_____. 1975b, Lawrence Berkeley Laboratory Report LBL-3650.

Mabuchi, H., Takahashi, H., Nakamura, Y., Notsu, K., and Hamaguchi, H. 1974, J. Inorg. Nucl. Chem., 36, 1687.

Martin, M. J. and Blichert-Toft, P. H. 1970, Nucl. Data Tables, 8, 1.

Matsuda, H., Umemoto, S., and Honda, M. 1971, Radiochim. Acta, 15, 51.

Meneguzzi, M., Cesarsky, C. J., and Meyer, J. P. 1975, Proc. 14th Int. Cosmic Ray Conf. (Munich), 12, 4183.

Meyer, J. P. and Reeves, H. 1977, Proc. 15th Int. Cosmic Ray Conf. (Plovdiv), 2, 137.

Mott, N. F. and Massey, H. S. W. 1965, The Theory of Atomic Collisions, 3d ed., Oxford, Clarendon Press.

Oppenheimer, J. R. 1928, Phys. Rev., 31, 349.

Perron, C. 1976, Phys. Rev., C14, 1108.

Pratt, R. H., Ron, Akiva, and Tseng, H. K. 1973, Rev. Mod. Phys., 45, 273.

Raisbeck, G. M. 1974, 2nd High Energy Heavy Ion Summer Study, ed. L. S. Schroeder, Lawrence Berkeley Laboratory Report LBL-3675, 333.

Raisbeck, G. M., Boerstling, P., Klapisch, R., Thomas, T. D. 1975, Phys. Rev., C12, 527.

Raisbeck, G. M., Crawford, H. J., Lindstrom, P. J., Greiner, D. E., Bieser, F. S., and Heckman, H. H. 1977a, Proc. 15th Int. Cosmic Ray Conf. (Plovdiv), 2, 67.

Raisbeck, G.M., Menninga, C., Brodzinski, R., and Wogman, N. 1977b, 15th Int. Cosmic Ray Conf. (Plovdiv), 2, 116.

Raisbeck, G. M., Perron, C., Toussaint, J., and Yiou, F. 1973, Proc. 13th Int. Cosmic Ray Conf. (Denver), 1, 534.

Raisbeck, G. M. and Yiou, F. 1971, Phys. Rev., A4, 1858.

_____. 1973, Proc. 13th Int. Cosmic Ray Conf., 1, 494.

_____. 1975a, Phys. Rev., C12, 915.

_____. 1975b, Phys. Rev. Lett., 35, 155.

_____. 1975c, Proc. 14th Int. Cosmic Ray Conf. (Munich), 2, 495.

_____. 1977, Proc. 15th Int. Cosmic Ray Conf. (Plovdiv), 2, 203.

Rao, M. N. 1970, Nucl. Data, B3-3, 4, 43.

Reames, D. V. 1974, in High Energy Particles and Quantas in Astrophysics. eds. F. B. Mc Donald and C. E. Fichtel (Cambridge:MIT Press), 54.

Renberg, P. U., Measday, D. F., Pepin, M., Schwaller, P., Favier, B., Richard-Serre, C. 1972, Nucl. Phys., A183, 81.

Roy, J. C. and Kohman, T. P. 1957, Canad. J. Phys., 35, 649.

Sauter, F. 1931, Ann. Physik, 9, 217.

Schneider, M. J. and Daehnick, W. W. 1971, Phys. Rev., C4, 1649.

Shapiro, M. M., Silberberg, R., and Tsao, C. H. 1975, Proc. 14th Int. Cosmic Ray Conf. (Munich), 2, 532.

Silberberg, R. and Tsao, C. H. 1973a, Ap. J. Suppl., 25, 315.

_____. 1973b, ibid., 25, 335.

_____. 1977, Proc. 15th Int. Cosmic Ray Conf. (Plovdiv), 2, 84.

Silberberg, R., Tsao, C. H., and Shapiro, M. M., 1976, in Spallation Nuclear Reactions and Their Applications, eds. B. S. P. Shen and M. Merker (Dordrecht-Holland:D. Reidel Publishing Co.), 49.

Slater, J. C. 1930, Phys. Rev., 36, 51.

Tsao, C. H., Shapiro, M. M., and Silberberg, R. 1973, Proc. 13th Int. Cosmic Ray Conf. (Denver), 1, 107.

Vatai, E. 1973, Nucl. Phys., A212, 413.

Verheul, H. 1970, Nucl. Data Sheets, B3-5, 6, 161.

Vervier, J. 1968, Nucl. Data, B2-5, 1.

Waddington, C. J. 1975, Proc. 14th Int. Cosmic Ray Conf. (Munich), 2, 521.

Wapstra, A. H. and Bos, K. 1977, At. & Nucl. Data Tables, 19, 177.

Webber, W. R., Leznick, J. A., Kish, J. C., and Simpson, G. A. 1977, Astrophys. Lett., 18, 125.

Yiou, F. and Raisbeck, G. M. 1970, Astrophys. Lett., 7, 129.

Yiou, F., Raisbeck, G. M., Perron, C., and Fontes, P. 1973, Proc. 13th Int. Cosmic Ray Conf. (Denver), 1, 512.

Zyranova, L. 1963, Once-Forbidden Beta-Transitions (Oxford:Pergamon Press).

TABLE 1: Effective Attachment Cross Sections and Correction Functions

	1 GeV/nuc		3 GeV/nuc		5 GeV/nuc	
Element	σ_{att} (mb/H atom)	f_{cor}	σ_{att} (mg/H atom)	f_{cor}	σ_{att} (mb/H atom)	f_{cor}
Be	.0073	.916	.0013	.915	.0007	.911
Ar	10.51	.710	1.86	.706	1.01	.689
Ca	17.26	.688	3.06	.684	1.65	.665
Ti	26.97	.667	4.77	.663	2.57	.643
V	33.19	.658	5.87	.653	3.15	.632
Cr	40.48	.648	7.16	.643	3.84	.622
Mn	48.95	.639	8.65	.634	4.63	.612
Fe	58.74	.631	10.38	.625	5.55	.603
Co	69.99	.622	12.36	.616	6.60	.593
Ni	82.84	.614	14.62	.608	7.79	.584

TABLE 2: Comparison at 530 MeV of the Proton-Nucleus Reaction Cross Section Measurements of Renberg et al. with Theory and Phenomenology.

Target[a]	Renberg et al. (mb)	Karol/f_k (mb)[b]	Bradt-Peters (mb)[c]
Be	195.4 ± 6.2	198.4 ± 5.0	191.7
B	213 ± 6	217 ± 8	220
C	233 ± 5	231 ± 2	238
O	290 ± 15	291 ± 3	294
Al	433.2 ± 7.7	428 ± 13	430
Fe	712 ± 13	732 ± 7	722
Cu	788 ± 17	793 ± 37	792
Ge	877 ± 18	862 ± 40	870
Sn	1201 ± 23	1203 ± 11	1229
Pb	1781 ± 46	1739 ± 18	1811
NaI	1704 ± 43	1599 ± 58	1670

[a] assumed to have isotopes in normal abundance

[b] using $f_k = 1.037 \pm .009$ (see eq. (43)) and Karol's formulae with the following constants: $\sigma_{pp} = 36.3$ mb, $\sigma_{pn} = 36.1$ mb, R_{rms} either from experiment or the equation $R_{rms} = .82\ A^{1/3} + .58$, c either from experiment or the equation $c = 1.07\ A^{1/3}$, and t either from experiment or the value 2.4. σ_{pp} and σ_{pn} are from Bugg et al. (1966) and experimental values of R_{rms}, c, and t are from de Jager et al. (1974).

[c] using the values $\sigma_o = 56$ and $b = 1.23$ given in Table 3.

TABLE 3: Fitting Parameters for Renberg et al. Data Using $\sigma = \sigma_o(1 + A^{1/3} - b)^2$

Parameter	Value
σ_o(mb)	56
b	1.23
$\langle(\delta\sigma_o)^2\rangle$	1.3
$\langle\delta\sigma_o\delta b\rangle$	3.3×10^{-2}
$\langle(\delta b)^2\rangle$	9.3×10^{-4}
χ^2	5.1*

*vs. 8 degrees of freedom (10 data points - 2 parameters)

TABLE 4: Comparison of Nucleus-Nucleus Reaction Cross Sections with Theory

Reaction	Kinetic Energy (GeV/nucleon)	Experiment (mb)[a]	Karol/f_k (mb)[b]
C - H	2.1	270 ± 14	266 ± 1
C - H	.87	260 ± 14	264 ± 1
He - H	2.1	111 ± 6	106 ± 2
He - H	.87	120 ± 6	105 ± 2
D - H	2.1	60 ± 16	72.5 ± .1
C - D	2.1	426 ± 15[c]	469 ± 1
C - D	.87	411 ± 21	466 ± 1
He - D	2.1	203 ± 8[c]	218 ± 2
He - D	.87	198 ± 10	216 ± 2
D - D	2.1	134 ± 8	141.3 ± .2
C - He	2.1	535 ± 19[c]	549 ± 6
C - He	.87	527 ± 20[c]	547 ± 6
He - He	2.1	276 ± 14	269 ± 3
He - He	.87	262 ± 18	268 ± 3
C - C	2.1	888 ± 44	954 ± 2
C - C	.87	939 ± 50	951 ± 2

[a] All measurements are from Jaros (1975). Note that the errors were obtained by adding Jaros' estimated systematic error of 5% to his tabulated statistical error.

[b] Using $f_k = 1.037 \pm .009$ (see text) and the same parameters as in Table 2 except that σ_{pp} = 47.2, 44.8 mb and σ_{pn} = 39.6, 43.1 mb for kinetic energies .87 and 2.1 GeV respectively, with σ_{pp} and σ_{pn} from Bugg et al. (1966).

[c] Weighted average of two measurement modes (both nuclei used as projectiles).

TABLE 5: Experimental Production Cross Sections for Proton-Nucleus Reactions at Energies Greater than 2.1 GeV/nucleon.

Fragment	Target					
	^{12}C[a,b]	^{13}C[b]	^{16}O[a]	^{24}Mg[c]	^{28}Si[c]	^{56}Fe[e]
^{6}Li	14.9 ±1.3*		13.9 ±2.4			17.3±5.2[e]
^{7}Li	11.0 ±1.0		11.1 ±1.3			19.0±5.7[e]
^{7}Be	9.2 ± .4	3.7±1.0	10.1 ±1.2	9.9± .9	10.7± .9	11.4±1.2
^{9}Be**	6.04± .46	6.4± .7	4.26± .55			8.1±1.2
^{10}Be	3.47± .30	5.9±1.7	2.05± .31			4.6± .8
^{10}B	19.3 ±3.0		10.7 ±1.7			5.4±1.6[e]
^{11}B	57.0 ±4.2		26.5 ±1.9			9.5±2.9[e]
^{12}C			34.3 ±4.8			
^{13}C			22.6 ±1.8			
^{14}C			3.69± .38			
^{14}N			31.8 ±3.2			
^{15}N			61.5 ±4.2			
^{22}Ne				31.5±3.9	18.2±2.6	7.4±1.5
^{45}Sc						18.0±1.9
^{46}Ti						27.5±7.5
^{48}Ti						25.1±5.6
^{49}V						18.6±3.2
^{50}V						10.0±1.6
^{51}V						2.9± .6
^{50}Cr						15.1±2.4
^{51}Cr						25.1±3.2
^{52}Cr						46 ±12
^{53}Cr						8.5±1.7
^{54}Cr						2.4±1.0
^{54}Mn						29.2±2.7

*All cross sections are in millibarns.

**Li9 branches to Be9 25% of the time.

References: (see text)

[a]Lindstrom et al. (1975b)

[b]Yiou et al. (1973)

[c]Raisbeck and Yiou (1975a) and semi-empirical

[d]Perron (1976) and semi-empirical

[e]Raisbeck et al. (1975) and semi-empirical to convert from Ni to Fe

TABLE 6a: Isotopes which, as Cosmic Rays, either have Half-Lives Greater than 1100 Years, or are EC Clocks.

Isotope	Lab $T_{1/2}$ (y)	Remarks*	CR $T_{1/2}$ (y)	Reference
^{10}Be	$(1.6\pm0.2)\times10^{6}$	β_-,555.8 max (100%), 3^+	$(1.6\pm0.2)\times10^{6}$	a,k
^{14}C	(5730±40)	β_-,156.6 max (100%), 1^+	(5730±40)	b,k
^{26}Al	$(7.2\pm0.3)\times10^{5}$	β_+,1174.0 max (82.1±2.5)%, 3^+ EC,1066.3 (2.7±.02)%, 3^+ EC,2196.0 (15.2±2.5)%, 3^+	$(8.8\pm0.5)\times10^{5}$	c,k
^{36}Cl	$(3.01\pm0.02)\times10^{5}$	β_-,709.6 max (98.1±0.1)%, 2^+ β_+122.2 max $(1.7\pm0.1)\times10^{-7}$%, 2^+ EC,1144.2, (1.9±0.1)%, 2^+	$(3.07\pm0.02)\times10^{5}$	c,k
^{40}K	$(1.28\pm0.01)\times10^{9}$	β_-,1311.6 max (89.33±0.11)%, 4^- β_+,483.0 max $(1.03\pm0.11)\times10^{-3}$%, 4^- EC,44.2 (10.67±0.11)%, 2^-	$(1.43\pm0.01)\times10^{9}$	c,k
^{41}Ca	$(1.06\pm0.09)\times10^{5}$	EC clock, see Appendix C	$(2.2\pm0.2)\times10^{5}$	d,e,f,k**
^{44}Ti	(47.3±1.2)	EC clock, see Appendix C	(100±3)	c,k
^{53}Mn	$(3.6\pm0.4)\times10^{6}$	EC clock, see Appendix C	$(7.7\pm0.9)\times10^{6}$	g,h,k**

*For $\beta_\pm$-decays, the endpoint energy (in keV) is given along with the mode's branching ratio and its change of spin and parity. For electron capture (EC), the energy (in keV) of the neutrino is given (ignoring binding). The remaining types of remarks should be self-explanatory.

**Used the weighted average $\langle T\rangle = W\ \Sigma T_i/\delta T_i^2$ and the root mean square error $\Delta T = W^{-1/2}$ max $\{1, [\Sigma(T_i-\langle T\rangle)^2/\delta T_i^2(n-1)]^{1/2}\}$, ^{i} where $W = \Sigma\ 1/\delta T_i^2$.

TABLE 6b:

Isotope	Lab $T_{1/2}$ (y)	Remarks	CR $T_{1/2}$ (y)	Reference
^{54}Mn		estimated 3^+ decay, see Appendix B	$[0.06 \text{ to } 10]\times10^6$	
^{60}Fe	$[1 \text{ to } 9]\times10^5$	β^-,150 max (100%), 2^+	$[1 \text{ to } 9]\times10^5$	i,k
^{56}Ni		estimated 3^+ decay, see Appendix B	$[0.1 \text{ to } 6]\times10^6$	
^{59}Ni	$(8\pm1)\times10^4$	EC clock, see Appendix C	$(1.7\pm0.2)\times10^5$	j,k

[a] Ajzenberg-Selove and Lauritsen (1974)
[b] Martin and Blichert-Toft (1970)
[c] Endt and Van der Leun (1973)
[d] Mabuchi et al. (1974)
[e] Emery et al. (1972)
[f] Drouin and Yaffe (1962) as corrected by Ref. d)
[g] Honda and Imamura (1971)
[h] Matsuda et al. (1971)
[i] Roy and Kohman (1957)
[j] Vervier (1968)
[k] Wapstra and Bos (1977)

TABLE 7: Cosmic Ray Abundances above the Atmosphere at Rigidities $R \gtrsim 4$ GV

Element	Abundance	Element	Abundance
Li	18±2	S	3±.4
Be	10.5±1	Cl	.5±.2
B	28±1	Ar	1.5±.3
C	100[a]	K	.8±.2
N	25±2	Ca	2.2±.5
O	91±2	Sc	.4±.2
F	1.7±.4	Ti	1.7±.3
Ne	16±2	V	.7±.3
Na	2.7±.4	Cr	1.5±.4
Mg	19±1	Mn	.9±.2
Al	2.8±1	Fe	10.8±1.4
Si	14±2	Co	.05±.02
P	.6±.2	Ni	.5±.1

[a]All ratios normalized to carbon.

Table 8a
THE ELEMENTAL MODIFICATION MATRIX FOR PROJECTILES BETWEEN Li AND P

	LI	BE	B	C	N	O	F	NE	NA	MG	AL	SI	P
LI	-547 22	37 8	33 6	28 2	27 6	28 3	32 7	29 5	31 7	29 5	31 6	28 6	31 6
BE	0 0	-618 26	25 4	20 1	18 4	18 2	18 4	18 3	18 4	18 2	18 4	19 2	18 4
B	0 0	0 0	-613 23	87 7	52 11	40 4	36 8	33 7	30 7	28 5	25 6	23 5	21 5
C	0 0	0 0	0 0	-663 29	76 17	63 7	38 9	34 7	29 7	26 5	22 5	20 4	18 4
N	0 0	0 0	0 0	0 0	-694 33	112 9	43 10	42 9	33 8	31 6	25 6	23 5	18 4
O	0 0	0 0	0 0	0 0	0 0	-732 36	118 23	89 14	68 12	62 9	51 9	47 8	37 7
F	0 0	0 0	0 0	0 0	0 0	0 0	-794 43	47 13	21 7	20 5	16 5	15 5	12 4
NE	0 0	0 0	0 0	0 0	0 0	0 0	0 0	-816 41	117 23	87 10	67 12	60 9	50 9
NA	0 0	0 0	0 0	0 0	0 0	0 0	0 0	0 0	-838 47	51 14	23 8	22 7	18 6
MG	0 0	0 0	0 0	0 0	0 0	0 0	0 0	0 0	0 0	-852 40	108 17	84 13	66 11
AL	0 0	0 0	0 0	0 0	0 0	0 0	0 0	0 0	0 0	0 0	-879 52	62 16	28 8
SI	0 0	0 0	0 0	0 0	0 0	0 0	0 0	0 0	0 0	0 0	0 0	-901 50	130 25
P	0 0	0 0	0 0	0 0	0 0	0 0	0 0	0 0	0 0	0 0	0 0	0 0	-949 58
S	0 0	0 0	0 0	0 0	0 0	0 0	0 0	0 0	0 0	0 0	0 0	0 0	0 0
CL	0 0	0 0	0 0	0 0	0 0	0 0	0 0	0 0	0 0	0 0	0 0	0 0	0 0
AR	0 0	0 0	0 0	0 0	0 0	0 0	0 0	0 0	0 0	0 0	0 0	0 0	0 0
K	0 0	0 0	0 0	0 0	0 0	0 0	0 0	0 0	0 0	0 0	0 0	0 0	0 0
CA	0 0	0 0	0 0	0 0	0 0	0 0	0 0	0 0	0 0	0 0	0 0	0 0	0 0
SC	0 0	0 0	0 0	0 0	0 0	0 0	0 0	0 0	0 0	0 0	0 0	0 0	0 0
TI	0 0	0 0	0 0	0 0	0 0	0 0	0 0	0 0	0 0	0 0	0 0	0 0	0 0
V	0 0	0 0	0 0	0 0	0 0	0 0	0 0	0 0	0 0	0 0	0 0	0 0	0 0
CR	0 0	0 0	0 0	0 0	0 0	0 0	0 0	0 0	0 0	0 0	0 0	0 0	0 0
MN	0 0	0 0	0 0	0 0	0 0	0 0	0 0	0 0	0 0	0 0	0 0	0 0	0 0
FE	0 0	0 0	0 0	0 0	0 0	0 0	0 0	0 0	0 0	0 0	0 0	0 0	0 0
CO	0 0	0 0	0 0	0 0	0 0	0 0	0 0	0 0	0 0	0 0	0 0	0 0	0 0
NI	0 0	0 0	0 0	0 0	0 0	0 0	0 0	0 0	0 0	0 0	0 0	0 0	0 0

XBL 789-10755

Table 8b

THE ELEMENTAL MODIFICATION MATRIX FOR PROJECTILES BETWEEN S AND Ni

	S	CL	AR	K	CA	SC	TI	V	CR	MN	FE	CO	NI
LI	29 6	35 5	30 5	33 6	32 6	41 8	44 7	49 10	45 8	49 10	40 8	51 11	43 7
BE	18 4	18 3	18 3	19 4	18 4	20 4	20 3	21 4	20 3	21 4	25 2	21 4	20 3
B	19 4	19 3	18 3	17 3	16 3	23 5	25 4	27 5	25 4	26 5	19 3	26 5	22 3
C	15 3	13 2	12 2	11 2	13 3	13 3	16 3	17 4	16 3	17 4	16 3	16 4	15 3
N	17 4	14 3	13 3	12 3	15 3	12 3	14 2	14 3	14 2	14 3	14 3	14 3	14 2
O	35 6	29 4	28 4	23 4	30 5	22 4	26 4	23 4	23 4	23 4	23 4	23 4	23 3
F	11 4	9 2	8 2	7 2	9 3	8 3	10 2	9 3	8 2	7 2	7 2	7 2	7 2
NE	46 8	38 6	35 6	30 5	37 7	28 5	32 4	28 5	27 4	24 4	24 3	22 4	22 3
NA	17 5	13 3	12 3	10 3	13 4	10 3	13 3	11 3	11 3	9 3	9 3	8 3	8 2
MG	60 10	48 7	44 7	37 6	45 7	34 6	39 5	34 6	33 5	29 5	28 4	24 4	24 3
AL	27 7	20 5	20 5	16 4	20 6	14 4	16 3	13 4	14 3	12 3	12 3	10 3	11 2
SI	102 18	66 10	64 10	52 9	62 11	46 9	52 7	45 8	42 7	37 7	36 6	31 6	32 5
P	58 17	22 6	21 6	18 5	23 7	15 5	16 4	13 4	14 4	12 4	12 3	10 3	12 3
S	-966 57	423 19	411 18	72 12	83 15	64 12	72 10	64 11	57 9	51 9	46 7	41 8	43 6
CL	0 0	-958 50	56 14	37 8	40 9	36 7	38 5	34 6	30 5	27 5	22 4	21 4	20 3
AR	0 0	7 2	-1001 55	111 19	115 20	61 12	69 10	56 10	57 9	48 9	47 8	41 8	41 6
K	0 0	0 0	0 0	-1045 63	56 16	53 10	58 8	51 9	45 7	40 7	35 6	31 6	28 4
CA	0 0	0 0	0 0	0 0	-1064 68	140 27	93 12	75 12	74 11	62 10	63 9	52 9	60 8
SC	0 0	0 0	0 0	0 0	0 0	-1123 76	33 6	33 8	27 6	23 7	21 2	19 5	18 4
TI	0 0	0 0	0 0	0 0	0 0	0 0	-1049 57	141 19	114 16	98 16	93 12	78 13	83 11
V	0 0	0 0	0 0	0 0	0 0	0 0	0 0	-1081 76	67 10	59 12	35 5	48 10	35 6
CR	0 0	0 0	0 0	0 0	0 0	0 0	0 0	0 0	-1125 57	121 17	111 13	90 15	68 13
MN	0 0	0 0	0 0	0 0	0 0	0 0	0 0	0 0	0 0	-1147 80	70 12	50 10	46 9
FE	0 0	0 0	0 0	0 0	0 0	0 0	0 0	0 0	0 0	27 22	-1161 77	184 31	133 17
CO	0 0	0 0	0 0	0 0	0 0	0 0	0 0	0 0	0 0	0 0	0 0	-1237 88	62 15
NI	0 0	0 0	0 0	0 0	0 0	0 0	0 0	0 0	0 0	0 0	0 0	0 0	-1224 63

XBL 789-10756

FIGURE CAPTIONS

Fig. 1a The simplified level scheme for the β_+ -decay of ^{56}Ni. Only those levels of ^{56}Co which can be reached by direct β_+ -decay are shown. All energies are in MeV and were taken from Auble (1977). The limit on the β_+ -branching ratio is from Rao (1970).

Fig. 1b The simplified level scheme for the β -decay of ^{54}Mn. Only those levels which can be reached by direct decay are shown. All energies are in MeV and were taken from Wapstra and Bos (1977). The limit on the β_+ -branching ratio is from Verheul (1970).

Fig. 2 A simplified chart of the nuclides for cosmic rays. The mass number A increases to the right and the atomic number increases towards the top. As in an earlier chart by Waddington (1975), the chart is folded (at A = 22 and A = 38). Each box represents a nuclide which requires explicit inclusion in propagation calculations (see text § I(b)). In each box, line 1 gives the mode(s) of decay and half-life, as a cosmic ray, line 2 gives the nuclide's total reaction cross section in the interstellar medium, and line 3 gives the non-trivial terms of the ν matrix (see text § II(g)).

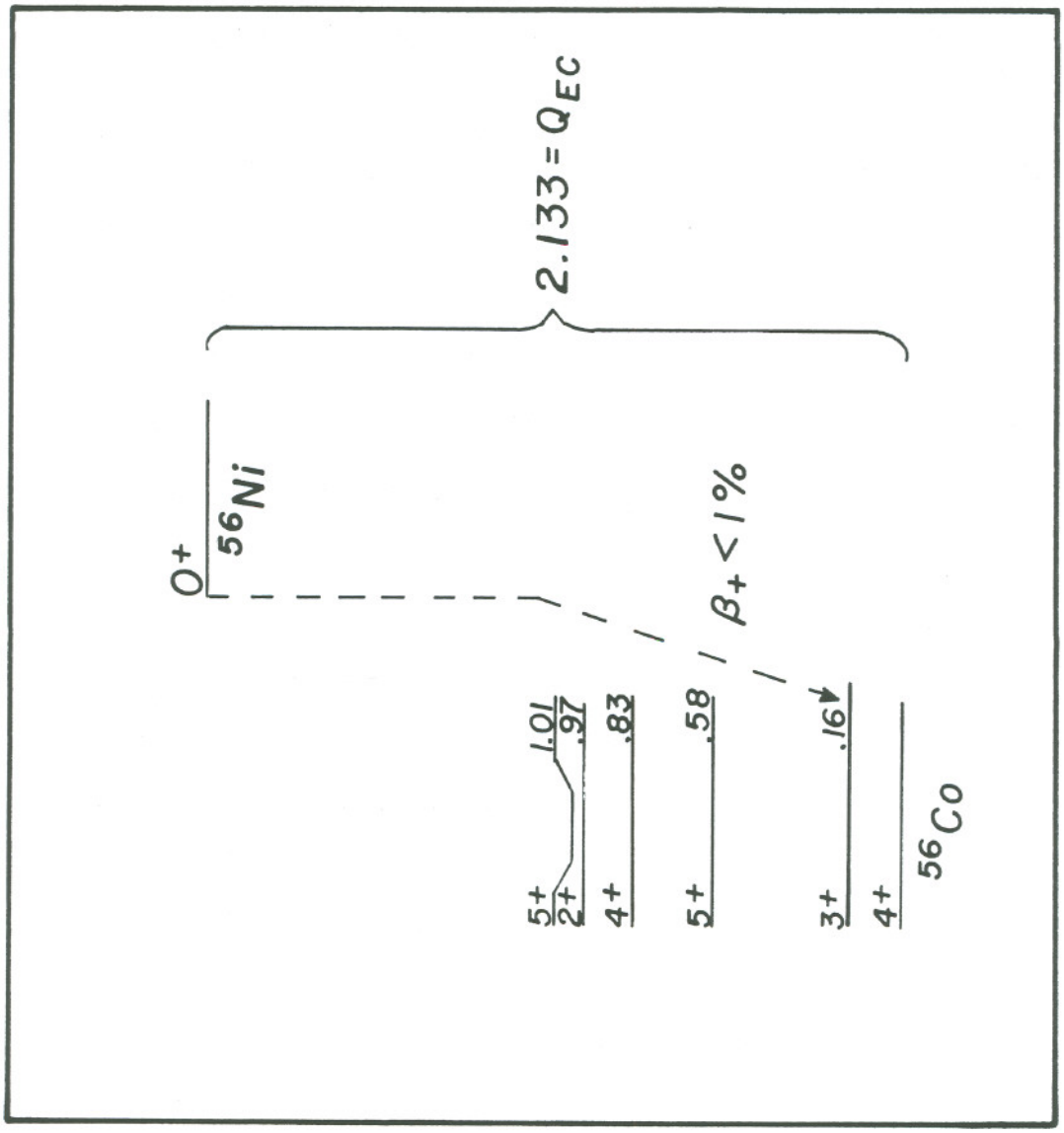

XBL 788-10019

Fig. 1a

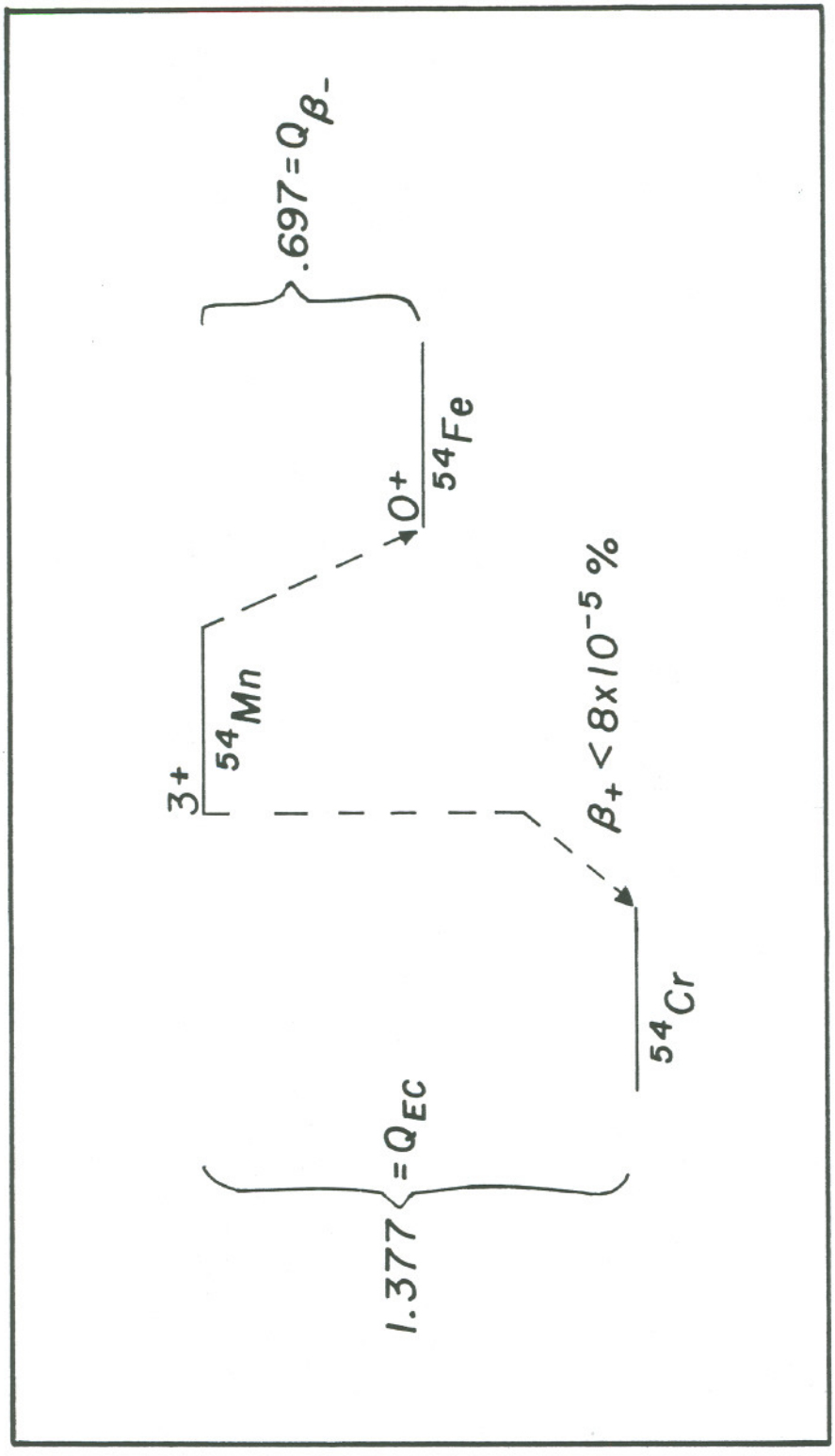

XBL 788-10020

Fig. 1b

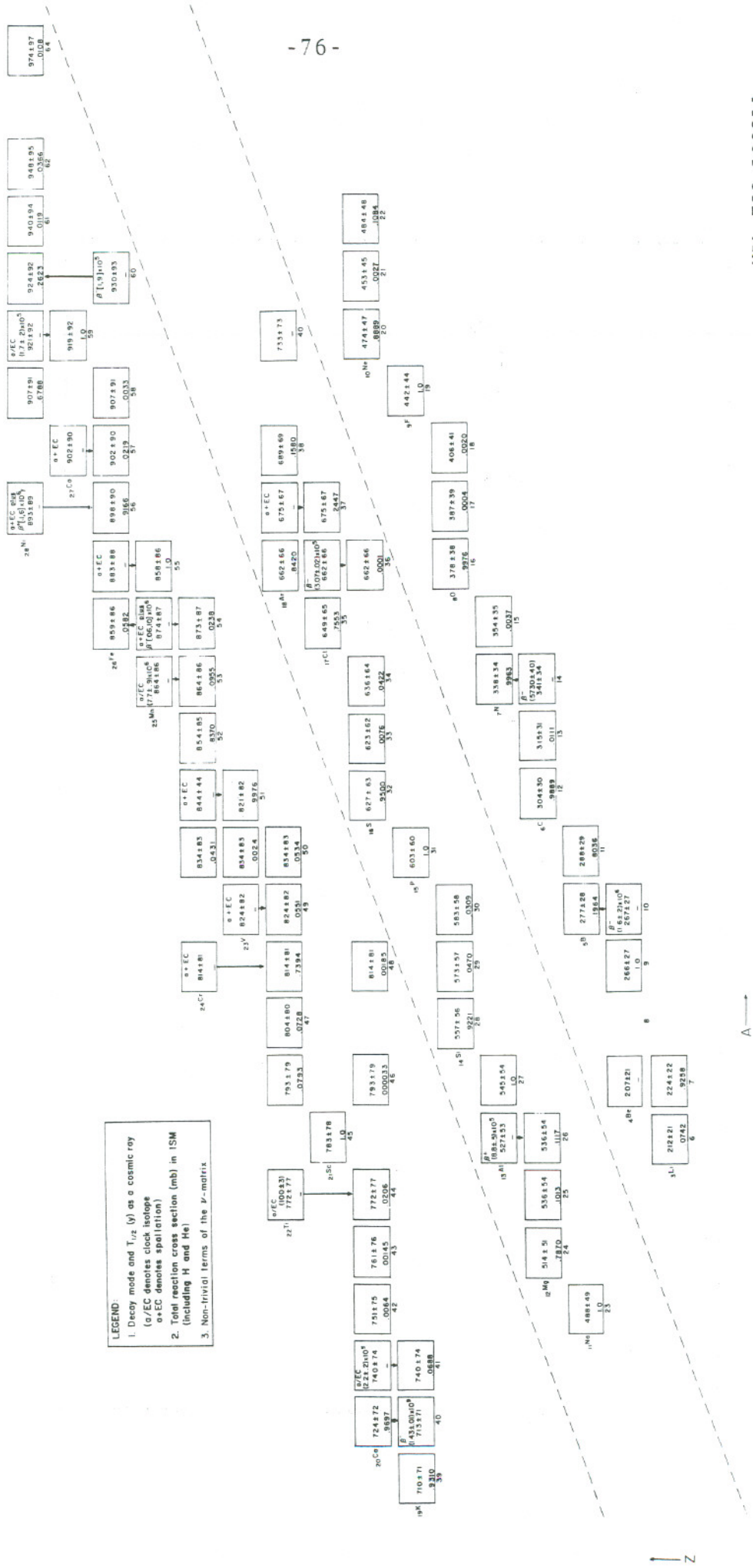

XBL 788-10021A

Fig. 2

Appendix A

As stated in § II(b), the stripping cross section can be more completely described as the total cross section for the loss of a K-shell electron by a hydrogenic atom following its collisions with the interstellar medium.

(a) Non-relativistic form

Dmitriev et al. (1966) have used the non-relativistic Born approximation to determine the stripping cross sections for arbitrary one-electron ions colliding with either hydrogen or helium atoms. They first break the cross section into two contributions - the elastic collisions in which the atom in the medium remains in its ground state and the inelastic collisions in which the atom in the medium does not remain in the ground state. In addition, each of these pieces is broken down into its contributions from close and distant collisions. The total cross section is the sum of their Eqs. (10) and (14) and for high (but non-relativistic) velocities ($\beta > 3 Z_{CR} \alpha$) can be approximated to within 10% by the expression

$$\sigma_{strip} = \frac{4\pi a_o^2 \alpha^2}{Z_{CR}^2 \beta^2} (Z_{med}^2 + Z_{med}) \qquad (A1)$$

$$\times \left[1 - \left(\frac{Z_{CR}}{\beta} \right)^2 \left(\frac{1 + Z_{med}/4}{1 + Z_{med}} \right) + \left(\frac{0.56}{1 + Z_{med}} \right) (Z_{med} \ln A + \ln B) \right]$$

where a_o is the Bohr radius,

α is the fine structure constant,

Z_{med} is the nuclear charge of the medium, and

Z_{CR} is the nuclear charge of the cosmic ray.

In addition, A and B are defined by the equations

$$A = \min(1.6\ \beta/Z_{CR}\ \alpha\ ,\ Z_{CR}/2\ Z_{med}^{*}) \quad ,$$

$$B = \min[(1.6\ \beta/Z_{CR}\ \alpha)\ (1 + 0.8\ u_s^{2}/Z_{CR}^{2})\ ,\ Z_{CR}/Z_{med}^{*}] \quad ,$$

where $Z_{med}^{*} = \left\{\begin{matrix} 1 & , \text{ for H} \\ 1.69, & \text{for He} \end{matrix}\right\}$ and

$$u_s = \left\{\begin{matrix} 1 & , \text{ for H} \\ 1.35, & \text{for He} \end{matrix}\right\} .$$

Note that the first factor in Eq. (A1) is just Bohr's expression for σ_{strip}. Also, Dmitriev et al. showed that only the first two terms within the brackets of Eq. (A1) arise from close collisions. Thus, Eq. (A1) will deviate from Bohr's formula if the logarithmic terms from distant collisions make a significant contribution.

Since explicit values for σ_{strip} are needed for $Z_{CR} > 18$ (see Fig. 2 and Table 1), and since the second term within its brackets is negligible for $\beta > 3\ Z_{CR}\ \alpha$, Eq. (A1) can be further approximated by the expression

$$\sigma_{strip} = \frac{4\pi a_o^{2}\ \alpha^{2}}{Z_{CR}^{2}\ \beta^{2}}\ (Z_{med}^{2} + Z_{med})\ [1 + 0.56\ \ln\ (1.6\ \beta/Z_{CR}\alpha)] \qquad (A2)$$

(b) Relativistic estimate

There is no directly applicable relativistic calculation for the loss of a K-shell electron. However, it is possible to reliably estimate the cross section if one adopts the following argument. First, view the collisions in the rest frame of the hydrogenic atom. Then if the velocity of the "incident" atom of the medium is sufficiently high, it should be possible to view its interactions with the hydrogenic atom as merely a superposition of the effect from the nuclear charge Z_{med} and Z_{med} times the effect from a single electron. In this way, the calculation reduces to properly weighting the relativistically correct expression for the ionization cross section due to the passage of a fast charged particle (instead of an atom). After some rearrangement of the ionization formula given in Mott and Massey (1965), this sum becomes

$$\sigma_{strip} = \frac{4\pi a_o^{\,2}\,\alpha^2}{Z_{CR}^{\,2}\,\beta^2}\; C_1 \left[\ln\left(\frac{4\,\beta^2\,\gamma^2}{C_2 Z_{CR}^{\,2}} \right) - \beta^2 \right] (Z_{med}^{\,2} + Z_{med}) \qquad \text{(A3)}$$

where the constants C_1 and C_2 have the values 0.285 and 0.048, respectively. Note that the $Z_{med}^{\,2}$ in Eq. (A3) reflects the contribution from the nucleus, while the Z_{med} stems from the electrons.

(c) Reliability of the estimate

In the limit of $\beta << 1$, Eq. (A3) becomes

$$\sigma_{strip} = \frac{4\pi a_o^2 \alpha^2}{Z_{CR}^2 \beta^2} (Z_{med}^2 + Z_{med}) [.99 + .57 \ln(1.6 \beta / Z_{CR}\alpha)] \qquad (A4)$$

which is virtually identical to Eq. (A2).

In conclusion, Bohr's formula is significantly in error (by more than a factor of 2) but can be corrected by properly including the effects of distant collisions. Equation (A3) is a much better approximation for the stripping cross section.

Appendix B

Cassé (1973a) has claimed that the variations in the nuclear matrix elements of "unique second-forbidden" decays (here denoted 3^+ decays) are limited enough to provide a means of predicting the lifetimes of ^{54}Mn and ^{56}Ni. This claim is checked below.

(a) Does there exist a "systematics" for 3^+ decays?

This section determines the amount of variation in the values of the nuclear matrix elements of those 3^+ transitions that are both well-determined and occur in nuclei with $A \leq 70$. The characteristics of the five transitions that meet these two requirements are given in Table B1. Note two changes from Cassé's Table I -- two additional branches for ^{26}Al and the removal of the ^{60}Co decay. The ^{60}Co case was removed on the basis of a review of the A = 60 chain (Kim 1975). Kim found that the two 3^+ branches of ^{60}Co were "very questionable" because the indirect arguments for them had been weakened by new data on electromagnetic transitions between excited levels in ^{60}Ni. That is, since a new line could cause the populating of the same levels as those that would be reached by the 3^+ decays, the β- branching ratios are no longer reliable.

As was discussed by Cassé (1973a,b) the reason for adding log $< S_2 >$ to log $(f_o T_*)$ in order to obtain log $(f_2 T_*)$ is to remove the variations caused by the energy-dependent part of the shape factor and to isolate the variations in the nuclear matrix elements themselves. Thus, if the values of the matrix elements were narrowly distributed, column (7) of Table B1 should have much less dispersion than column (5).

That is clearly not the case. Note particularly the $\log(f_2T_*)$ values for the three ^{26}Al cases. Since the last two transitions differ only in the mode of decay, their equal $\log(f_2T_*)$ values show that the variations in matrix elements have been isolated. However, that common value differs from that of the first ^{26}Al transition by more than an order of magnitude, even though the matrix elements involve the same initial states. Thus there is no sound basis for the claim that the dispersion in $\log(f_2T_*)$ is small.

(b) The 3^+ half-lives for ^{54}Mn and ^{56}Ni

As seen above, the large dispersion in both the $\log(f_oT_*)$ and the $\log(f_2T_*)$ values makes calculations with the distribution's averages unreliable. However, one can hope that the dispersion for all 3^+ decays is no larger than that seen in Table B1. There are two possibilities: (1) that the table's range of $\log(f_oT_*)$ values brackets those of other 3^+ decays and (2) that it is the range of $\log(f_2T_*)$ that brackets the others. In case (1) the range of 12.75 to 14.22 in the $\log(f_oT_*)$ values of Table B1 leads to the ranges in deduced $T_{1/2}$'s shown in the second column of Table B2, while in case (2), the range of 10.89 to 12.74 in the $\log(f_oT_*)$ values leads to the values shown in the third column. Strictly speaking, these estimates apply only to the lifetimes in the laboratory since the integrated statistical factor was determined from a screened Fermi function. However, since the lifetimes turn out to have such a large range, the relatively small modifications that would be introduced by the removal of screening effects have been neglected

in this work. Thus, taking the union of the two sets of lifetime ranges gives the final limits shown in Table 6. That means, for example, that the half-life of the positron branch of ^{54}Mn might lie anywhere in the interval from 6×10^{6}y to 8×10^{9}y.

TABLE B1: Characteristics of Well-determined "Unique Second Forbidden Transitions" with $A \leq 70$.

Transition	$T_{1/2}$ (y)	E[a] (KeV)	Branch (percent)	$\log(f_o T_*)$[b]	$\log\langle S_2\rangle$[c]	$\log(f_2 T_*)$[d]	Reference
$^{10}Be(0^{+-}\rightarrow 3^{+})$	$(1.6\pm0.2)\times10^{6}$	555.8±0.8	100	13.51±.05	-2.62	10.89	e,f
$^{22}Na(3^{++}\rightarrow 0^{+})$	2.602±0.002	1820.3±0.5	$(6\pm1)\times10^{-2}$	12.75±.07	- .92	11.83	e,g
$^{26}Al(5^{+}\xrightarrow{EC}2_2^{+})$	$(7.2\pm0.3)\times10^{5}$	1066.3±0.5	(2.7±.2)	13.33±.04	-1.78	11.55	e,g
$^{26}Al(5^{++}\rightarrow 2_1^{+})$	$(7.2\pm0.3)\times10^{5}$	1174.0±0.5	(82.1±2.5)	14.22±.02	-1.51	12.71	e,g
$^{26}Al(5^{+}\xrightarrow{EC}2_1^{+})$	$(7.2\pm0.3)\times10^{5}$	2196.0±0.5	(15.2±2.5)	13.19±.07	- .45	12.74	e,g

[a] Note that for the β decays, E is the maximum kinetic energy of the beta particles.

[b] $T_{1/2}$ is the effective half-life $\equiv T_{1/2}/r$, where r is the branching fraction. The integrated statistical factor, f_o, is from Gove and Martin (1971) and incorporates both screening and the effects of the finite size of the nucleus.

[c] Obtained from a quadratic interpolation in the tables of Zyranova (1963).

[d] Defined by $\log(f_2 T_*) = \log(f_o T_*) + \log\langle S_2\rangle$.

[e] Wapstra and Bos (1977).

[f] Ajzenberg-Selove and Lauritsen (1974).

[g] Endt and Van der Leun (1973).

TABLE B2: Possible Half-lives for the 3^+ Decays of ^{54}Mn and ^{56}Ni

Transition	Intervals for $T_{1/2}$ If[a] $12.75 \leq \log (f_o T_*) \leq 14.22$	If[a,b] $10.89 \leq \log (f_2 T_*) \leq 12.74$	$\log \langle S_2 \rangle$[c]	Reference
^{54}Mn $(3^+ \pm 0^+)$	$[.059, 1.7]\times10^8$ y	$[1.1, 80]\times10^8$ y	-1.81	d
^{54}Mn $(3^+ \mp 0^+)$	$[.065, 1.9]\times10^6$ y	$[.14, 9.8]\times10^6$ y	-3.14	d
^{56}Ni $(0^+ \pm 3^+)$	$[.098, 2.9]\times10^6$ y	$[.087, 6.3]\times10^6$ y	-2.19	d,e

[a] Log f_o from Gove and Martin (1971) and the endpoint energies given in text (Fig. 1)

[b] Defined by $\log (f_2 T_*) = \log (f_o T_*) + \log \langle S_2 \rangle$.

[c] Obtained from a quadratic interpolation in the tables of Zyranova (1963).

[d] Wapstra and Bos (1977).

[e] Schneider and Daehnick (1971).

Appendix C

Since a fast nucleus has at most one K-shell electron, its half-life via electron capture will as a first approximation be twice as great as that observed in the lab. In addition there are two smaller effects -- an increase in the half-life because there are no captures from the higher shells and a decrease because the fast nucleus is unscreened. The magnitude of these effects is determined below for the 2^-, 1^+, 2^+, and 2^+ decays of the isotopes ^{41}Ca, ^{44}Ti, ^{53}Mn, and ^{59}Ni, respectively.

(a) Captures from the higher shells

Following Martin and Blichert-Toft (1970) (denoted MB), let ϵ denote the full rate for decay by electron capture and let ϵ_x, denote the partial rate for capture of an electron from the x-th shell ($x=K,L_1,L_2,L_3,M,N,\ldots$). Then it is convenient to write

$$\frac{\epsilon}{\epsilon_K} = 1 + \frac{\epsilon_{L_1}}{\epsilon_K}\left[1 + \frac{\epsilon_{L_2} + \epsilon_{L_3}}{\epsilon_{L_1}}\right] + \frac{\epsilon_{L_1}}{\epsilon_K}\left[\frac{\epsilon_{MN\ldots}}{\epsilon_{L_1}}\right] \quad . \qquad (C1)$$

For both allowed and unique forbidden transitions, i.e. for ^{41}Ca and ^{44}Ti, only a single nuclear matrix element contributes to an ϵ_x. This "uniqueness" means that any ratio of the ϵ_x's is independent of the matrix element and is only a function of the Z of the parent nucleus and the momentum of the outgoing neutrino. In the case of the 2^+ decays of ^{53}Mn and ^{59}Ni, the decay rates for each shell depend on differing linear combinations of three different matrix elements.

However, Vatai (1973) has used the β-decay formalism of Behrens and Buhring (1971) to show that, even for non-unique transitions, the ratios of ϵ_x's for shells having the same total angular momentum are independent of the nuclear matrix elements. He also showed a reasonable preliminary estimation of other ratios could be obtained by assuming that they too were independent of the nuclear matrix elements. For the cases of ^{53}Mn and ^{59}Ni, such estimates show that the sum of the ratios $\epsilon_{L_3}/\epsilon_{L_1}$ and $\epsilon_{M_3}/\epsilon_{L_1}$ contribute only ~.1% to the final ϵ/ϵ_K. Thus for calculating the importance of captures from higher shells this work will treat all ratios of ϵ_x's as if they were independent of nuclear matrix elements. The results obtained from Eq. (C1) by using the tables in MB plus the momentum of a transition's outgoing neutrino are given in Table C1.

In the decay of a neutral atom one is unable to distinguish experimentally between a direct capture of the K-shell electron and an L-shell capture, if the L-shell vacancy is filled during the transition by a K-shell electron. In addition to such "exchange effects," there is an imperfect atomic overlap because of the different nuclear charge seen by the initial and final atomic states. Thus in the notation of MB, the experimental K-capture rate is given by

$$\epsilon_K = \epsilon_K^{\,o}\, B_K \qquad \text{(C2)}$$

where $\epsilon_K^{\,o}$ is the "pure" capture rate and B_K is the correction due to the exchange and overlap effects. Table C1 gives the values for B_K (according to MB) and also shows that the decay rate of a neutral atom is approximately 10% greater than the rate due to "pure" K-capture.

(b) The effects of screening

Once the neutral atom's "pure" capture rate for the K-shell has been determined, the remaining differences between the lab decay rate and its decay rate as a cosmic ray arise from a rate's small dependence upon screening. Recall that (cf. Konopinski and Rose 1965) in the normal approximation the K-shell capture rate for any transition with $\Delta I > 0$ depends on the product of g_K^2, the square of the large component of the electron's radial wave function at the nuclear surface, $(q_K^2)^{\Delta I}$ (q_K is the momentum of the outgoing neutrino), and other factors that are independent of the number of electrons attached to a nucleus. Thus, values are required of the ratios $(g_K^u)^2/g_K^2$ and $(q_K^u)^{2\Delta I}/q_K^{2\Delta I}$, where the superscript u denotes a quantity's value in the unscreened case.

Since for $Z < 30$, the effect of the finite size of the nucleus is negligible (cf. Konopinski and Rose 1965), the effect on g_K due to screening can be computed by comparing the values given by MB with those obtained for g_K by assuming a point-Coulomb potential. The unscreened result can be found analytically and is given by the equation (cf. Bjorken and Drell 1964)

$$g_K^u = 2(Z\alpha)^{3/2} \left\{ [(1+\gamma)/\Gamma(1+2\gamma)]^{\frac{1}{2}} (2Z\alpha R)^{\gamma-1} e^{-Z\alpha R} \right\} \qquad \text{(C3)}$$

where $\gamma = \sqrt{1-(Z\alpha)^2}$, R is the nuclear radius, the units are $\hbar = c = m_e = 1$, and the term in brackets shows the change from the non-relativistic case. Table C2 provides the values of the ratio $(g_K^u)^2/g_K^2$ for the same isotopes that appear in Table C1.

The effect on q_K arises from the calculation of the energy difference between initial and final states. In the neutral atom, Bahcall (1963) showed that K-capture is really the production of a K-shell vacancy in the daughter atom so that

$$q_K = Q_a - E_f - w'_K \tag{C4}$$

where Q_a is the atomic mass difference, E_f is the (non-negative) difference between the ground state of the daughter nucleus and the actual level reached by the transition, and w'_K is the (positive) binding energy of a K-shell electron in the daughter nucleus. In the unscreened case, q_K^u is given by the equation

$$q_K^u = Q_n - E_f + m_e - w_K^u \tag{C5}$$

where Q_n is the nuclear mass difference and w_K^u is the (positive) binding energy of a K-shell electron in the parent nucleus. However, for electron capture (where the daughter nucleus has one less proton)

$$Q_a = Q_n + m_e + E_e(Z) - E_e(Z-1), \tag{C6}$$

where $E_e(Z)$ is the (negative) total electric energy for an atom of Z electrons. Also for a point-Coulomb potential the ground state energy is given by the equation

$$w_K^u = m_e[1-(1-Z^2\,\alpha^2)^{\frac{1}{2}}] \quad . \tag{C7}$$

Substituting Eqs. (C6) and C7) into (C5) gives the equation

$$q_K^u = Q_a + E_e(Z-1) - E_e(Z) - E_f - m_e[1-(1-Z^2\,\alpha^2)^{\frac{1}{2}}] \quad . \tag{C8}$$

Since the transition energy $(Q_a - E_f)$ is much larger than the K-shell binding energies w_K^u and w'_K, Eqs. (C4) and (C8) mean that the ratio q_K^u/q_K is given by the expression

$$\frac{q_K^u}{q_K} = 1 + \frac{w'_K - (w_K^u - E_e(Z-1) + E_e(Z))}{Q_a - E_f} \qquad \text{(C9)}$$

As shown in Table C2, Eq. (C9) shows that q_K^u/q_K differs from unity by less 3 parts in a thousand for the isotopes of interest.

(c) Final determination of the half-lives

Let ϵ_{CR} denote the decay rate for a fast nucleus with one K-shell electron. Then, as discussed above, ϵ_{CR} is just the product of one-half of the rate for "pure" K-capture in the lab and the appropriate ratios of screened and unscreened quantities. That is,

$$\epsilon_{CR} = \tfrac{1}{2} \left[\frac{\epsilon_K^o}{\epsilon}\right] \left[\frac{(g_K^u)^2}{g_K^2}\right] \left[\frac{(q_K^u)^{2\Delta I}}{q_K^{2\Delta I}}\right] \epsilon \qquad \text{(C10)}$$

It was also shown that the ratio of the q_K's is essentially unity. Thus, Eq. (C9) means that the half-life for electron capture by a fast nucleus, $T_{1/2,CR}$, is given by the expression

$$T_{1/2,CR} = 2\, T_{1/2,Lab}(\epsilon/\epsilon_K^o)/[(g_K^u)^2/g_K^2] \quad . \qquad \text{(C11)}$$

where $T_{1/2,Lab}$ is the neutral atom half-life. Eq. (C11) and Tables C1 and C2 were used to generate the half-lives shown in Table 6.

TABLE C1: The Ratio of all Electron Captures to those from the K-shell.

Isotope	ΔI^{π} [a]	q_K^2 [b]	$q_{L_1}^2$ [b]	$\varepsilon/\varepsilon_K$ [c]	B_K [d]	$\varepsilon/\varepsilon_k$ [o]
^{41}Ca	2^-	0.6682	0.6784	1.115	0.982	1.095
^{44}Ti	1^+ [e]	0.0495	0.0531	1.124	0.982	1.104
^{44}Ti	1^+ [f]	0.1413	0.1473	1.120	0.892	1.100
^{53}Mn	2^+	1.3344	1.3585	1.124	0.985	1.107
^{59}Ni	2^+	4.3493	4.4050	1.127	0.986	1.111

[a] $\Delta I = |I_i - I_f|$, $\pi = \pi_i \pi_f$ where I denotes the spin, π denotes the parity of the nuclear level and i(f) denotes initial (final).

[b] $q_z = Q_a - E_f - w_x'$ is the neutrino's momentum where w_x' is the binding energy of an electron in the x-th shell of the daughter nucleus, Q is the atomic mass difference from Wapstra and Bos (1977), E_f is the difference between the final level and the ground state energy of the daughter nucleus, and all quantities are expressed in units of $m_e c^2$.

[c] From equation (C1) and the formulas given in Martin and Blichert-Toft (1970).

[d] Exchange and overlap correction (see text).

[e] Branches (98.1 1.5)% to a level 146.25 keV above the ^{44}Sc ground state (Endt and Van der Leun 1973).

[f] Branches (1.9 1.5)% to a level 67.85 keV above the ^{44}Sc ground state (Endt and Van der Leun 1973).

TABLE C2: The Effects of Screening on the Large Components of the K-shell's Radial Wave Function

Isotope	g_K^{b}	g_K^{u} [a]	$(g_K^u)^2/g_K^2$	$(q_K^u/q_K)-1$ [c]
^{41}Ca	.1169	.1195	1.045	5×10^{-4}
^{44}Ti	.1367	.1397	1.044	3×10^{-3} [d]
^{44}Ti	.1367	.1397	1.044	2×10^{-3} [e]
^{53}Mn	.1728	.1694	1.041	5×10^{-4}
^{59}Ni	.2097	.2057	1.039	4×10^{-4}

[a] g_K^u is the unscreened function obtained from Eq. (C2) with R given by the equation (Martin and Blichert-Toft 1970)

$$R = (.002908A^{1/3} - .002437A^{-1/3})\ \hbar/m_e c.$$

[b] From Martin and Blichert-Toft (1970).

[c] From equation (C8), using atomic mass differences from Wapstra and Bos (1977), w'_K and $E_e(Z)$ from Huang et al. (1976), and in the case of ^{44}Ti, values for E_f are from Endt and Van der Leun (1973).

[d] For the 98.1% branch.

[e] For the 1.9% branch.

APPENDIX D

This appendix provides the detailed manipulations involved in computing the errors on each term in the elemental modification matrix.

Since the elemental modification matrix is actually defined via its inverse, the formula connecting perturbations in a matrix with those in its inverse is needed. Let B be any invertible matrix. Then since $B\ B^{-1} = 1$,

$$\delta B_{IJ} (B^{-1})_{JK} + B_{IJ}(\delta B^{-1})_{JK} = 0 \qquad \text{(D1)}$$

where δB_{IJ} is the perturbation in B_{IJ}, $(\delta B^{-1})_{JK}$ is the perturbation in $(B^{-1})_{JK}$, and the summation convention has been used for the sum over J. Using Eq. (D1), the Eq. for $\delta \mathscr{M}_{IL}$ becomes

$$\delta \mathscr{M}_{IL} = - \mathscr{M}_{IJ} (\delta \mathscr{M}^{-1})_{JK} \mathscr{M}_{KL} \quad . \qquad \text{(D2)}$$

Using Eq. (55) and assuming no uncertainty in the ν's, the equation for $(\delta \mathscr{M}^{-1})_{JK}$ becomes

$$(\delta \mathscr{M}^{-1})_{JK} = \sum_j (\delta M^{-1})_{jm} \nu_{mK} \quad . \qquad \text{(D3)}$$

After substituting Eq. (D3) into Eq. (D2) and using Eq. (D1) for $(\delta M^{-1})_{jk}$, Eq. (D2) takes the form

$$\delta \mathscr{M}_{IL} = R_{Ik} \delta M_{k\ell} T_{\ell L} \ , \qquad \text{(D4)}$$

where the rectangular matrices R and T are defined by the expressions

$$R_{Ik} = \mathscr{M}_{IJ} \sum_j (M^{-1})_{jk} \tag{D5}$$

and

$$T_{RL} = (M^{-1})_{\ell m} \nu_{mk} \mathscr{M}_{KL} \quad . \tag{D6}$$

Thus, the mean square error in the term $\mathscr{M}_{IL}$ is given by the expression

$$\langle (\delta \mathscr{M})^2_{IL} \rangle = R_{Ik} R_{Ik'} \langle \delta M_{k\ell} \, \delta M_{k'\ell'} \rangle T_{\ell L} \, T_{\ell' L} \tag{D7}$$

where $\langle \delta M_{k\ell} \, \delta M_{k'\ell'} \rangle$ is the covariance matrix for M. Recall that the modification matrix is the sum of three matrices, F, D, and E, that involve different physical processes, so that $\langle \delta F_{k\ell} \, \delta D_{k'\ell'} \rangle = 0$ and similarly for the other two averages of terms from different matrices. However, there can be correlations among elements within each array. These correlations are computed below.

In principle the correlations of the matrix F can come from either the total reaction cross sections or the partial fragmentation cross sections. It was shown in § II(d) that the total reaction cross sections are generated by formulae that involve the nuclear charge distributions of the projectile and target. Moreover, an interpolation formula for the distributions was used whenever measurements were unavailable. Thus, in practice many of the terms are correlated. However, this fact will be ignored in accordance with

the assumption that actual measurements would randomly scatter about the results of the interpolation formula and destroy this "artificial" correlation. Thus in this work it will be assumed that the diagonal terms are neither correlated with each other nor with the off-diagonal terms. As discussed in § II(e), most of the off-diagonal terms of F are given by the semi-empirical formulae of Silberberg and Tsao and thus have some correlation. However, the simplifying assumption will be made that there is no mean correlation for different off-diagonal terms, whether experimental or semi-empirical. Thus the form

$$\langle \delta F_{k\ell} \, \delta F_{k'\ell'} \rangle = \langle \delta F_{k\ell}{}^2 \rangle \, \delta_{kk'} \, \delta_{\ell\ell'} \, , \tag{D8}$$

will be used with the error estimates given in § II(d) and (e), and where $\delta_{kk'}$ and $\delta_{\ell\ell'}$ are Kronecker deltas.

Non-zero terms in D (the matrix of long-lived decays) are correlated even if the lifetimes of the unstable species are uncorrelated. These correlations stem from the fact that the effects of a decay are incorporated twice, both as a diagonal term (with a minus sign) and as an off-diagonal term (with a plus sign). For definiteness, assume that the k_o-th entry of M decays to the ℓ_o-th entry with a mean life τ_{k_o}. Then if $\langle \delta \tau_{k_o}{}^2 \rangle$ is the mean square error given in Table 6, the correlation coefficient for D becomes

$$\langle \delta D_{k\ell}\ \delta D_{k'\ell'} \rangle = \sum_{k_o} \delta_{\ell k_o}\ \delta_{\ell' k_o}\ (\delta_{k\ell_o} - \delta_{kk_o})(\delta_{k'\ell_o} - \delta_{k'k_o})$$

$$\times \frac{\langle \delta\tau_{k_o}{}^2 \rangle}{(\gamma v \tau_{k_o}{}^2)^2} \qquad \text{(D9)}$$

where the sum over k_o represents the search through Table 6 and the extensive string of Kronecker deltas both represents the fact that only terms from the same physical decay are correlated (the first two factors) and keeps the bookkeeping straight on the net sign of the correlation.

In principle, terms in E are correlated in the same manner as the terms in D. However, as discussed in § II(b), the errors in the attachment cross sections are negligible. Thus only the correlations for the 4 cases that require stripping cross sections are needed. Once again assume that the k_o-th entry of M is the one-electron state of an electron that decays to the ℓ_o-th entry of M. Then if $\langle \sigma_{strip,k_o} \rangle^2$ is the mean square error discussed in § II(b), the correlation coefficient for E is virtually identical to Eq. (D9), namely

$$\langle \delta E_{k\ell}\ \delta E_{k'\ell'} \rangle = \sum_{k_o} \delta_{\ell k_o}\ \delta_{\ell' k_o} (\delta_{k\ell_o} - \delta_{kk_o})(\delta_{k'\ell_o} - \delta_{k'k_o})$$

$$\times n_H{}^2 \langle \delta\sigma_{strip,k_o}{}^2 \rangle \qquad \text{(D10)}$$

where the sum over k_o represents the search over the 4 possibilities.

In summary,

$$\langle \delta M_{k\ell}\ \delta M_{k'\ell'} \rangle = \langle \delta F_{k\ell}\ \delta F_{k'\ell'} \rangle + \langle \delta D_{k\ell}\ \delta D_{k'\ell'} \rangle + \langle \delta E_{k\ell}\ \delta E_{k'\ell'} \rangle \qquad \text{(D11)}$$

with $\langle \delta F_{k\ell}\ \delta F_{k'\ell'} \rangle$, $\langle \delta D_{k\ell}\ \delta D_{k'\ell'} \rangle$, and $\langle \delta E_{k\ell}\ \delta E_{k'\ell'} \rangle$ given by Eqs. (D8), (D9), and (D10), respectively. Substituting Eq. (D11) into Eq. (D7) expresses the errors in $\mathcal{M}$ in terms of the quantities discussed in § II. These errors are given in Table 8.